1-1-2009

Effect of Electrical Charges on Glycerol Nanodroplets Catalytic Reforming

Gayan I. Nawaratna

EFFECT OF ELECTRICAL CHARGES ON GLYCEROL NANODROPLETS CATALYTIC REFORMING

By

Gayan I. Nawaratna

A Thesis
Submitted to the Faculty of
Mississippi State University
in Partial Fulfillment of the Requirements
for the Degree of Master of Science
in Biological Engineering
in the Department of Agricultural and Biological Engineering

Mississippi State, Mississippi

August 2009

EFFECT OF ELECTRICAL CHARGES ON GLYCEROL NANODROPLET CATALYTIC REFORMING

By

Gayan I. Nawaratna

Approved:

Sandun Fernando Assistant Professor of Agricultural and Biological Engineering (Director of Thesis)	Lester Pordesimo Assistant Professor of Agricultural and Biological Engineering (Co-Director of Thesis)
Radhakrishnan Srinivasan Assistant Professor of Agricultural and Biological Engineering (Committee Member and Graduate Coordinator)	S.D. Fillip To Associate Professor of Agricultural and Biological Engineering (Committee Member)
James Warnock Assistant Professor of Agricultural and Biological Engineering (Committee Member)	Sarah A. Rajala Dean of Bagley College of Engineering

Name: Gayan I. Nawaratna

Date of Degree: August 8, 2009

Institution: Mississippi State University

Major Field: Biological Engineering

Major Professor: Dr. Sandun Fernando

Title of Study: EFFECT OF ELECTRIAL CHARGES ON GLYCEROL NANODROPLET CATALYTIC REFORMING

Pages in Study: 71

Candidate for Degree of Master of Science of Biological Engineering

Recently there has been increasing interest in using glycerol as a substrate on steam reforming due to the increase of biodiesel production. With the increase of biodiesel production a glut of glycerol has resulted and this would be a more suitable substrate for value added production of hydrogen from reforming. Reforming biorenewable viscous fluids such as glycerol is difficult due to mass transfer limitations associated with vaporizing glycerol to gas phase before steam reforming.

This study was to evaluate the feasibility of reforming electrically atomized liquid phase glycerol by means of a technique called electro-spray. It was hypothesized that reforming electrically charged glycerol nanodroplets on an oppositely charged conductive catalyst will increase the reforming performance as opposed to a neutral catalyst-substrate system. Hydrogen yield, selectivity was increased by 20%, 25% respectively when nanodroplets introduced. Exerting an electrical charge to the substrate-catalytic system significantly enhanced the reforming performance irrespective of the physical phase.

ACKNOWLEDGMENTS

I acknowledge my profound sense of gratitude and indebtedness to my research advisor Dr. Sandun D. Fernando, Assistant Professor, Department of Biological and Agricultural Engineering, Texas A&M University for his inspiring, helpful suggestions and persistent encouragements as well as close and consistent supervision throughout the period of my Masters program. I shall forever remain grateful for the lessons learned at the hand of such a gifted and revered mentor.

I would like to express my sincere gratitude to my co-major supervisor Dr. Lester Pordesimo, and committee member Dr. Radhakrishnan Srinivasan for their suggestions in order to complete the research. My sincere thanks also go to the entire faculty in the Department of Agricultural and Biological Engineering for their support. I would like to thank Ms. Sharron Miles and Kimberly young, Department staff, for their help with all the paper work related to my study and research.

I would like to extend my deep gratitude to all the bioenergy group members: Dr. Agus Haryanto, Dr. Shushil Adhikari, Dr. Alok K. Singh, Saroj K. Jha, Dr. Shetian Liu, Dr. Xuejun Ye, and Anuradh Gunawardena. Special thanks go to Dr. Shetian Liu for build the reforming unit. Last but not least, I gratefully acknowledge the affection and moral support I received from my family throughout my life.

TABLE OF CONTENTS

LIST OF TABLES

LIST OF FIGURES

CHAPTER I

INTRODUCTION

The ever increasing demand for energy and drastic depletion of fossil fuels has impelled research community to search for alternate energy sources. Hydrogen is widely considered as one of the most promising alternate energy sources mainly in the context of providing mobile power[1, 2]. Extensive use of hydrogen as an energy carrier could help alleviate concerns related to energy security, air quality and global climate change. Also, hydrogen is beneficial because the byproducts of hydrogen conversion are generally benign for human health and the environment [1].

Hydrogen can be produced from domestically available substrate sources including fossil fuels, renewables, and nuclear power. When it comes to renewable sources, hydrogen has been produced by several methods including gasification, steam reforming, aqueous phase reforming, and partial oxidation. Among these, steam reforming of oxygenated hydrocarbons is the most widely used when the substrates are in liquid phase/vapor phase [1, 3, 4]. Gasification is presently limited to solid substrates. Aqueous phase reforming is the most recent concept and is still the subject of much research and development [5-8].

1.1 Problem Statement

As stated earlier, hydrogen is mainly produced via steam reforming of fossil fuel gases [1, 4, 9] but a wealth of other renewable CO_2 neutral raw materials such as lipids, carbohydrates and their derivatives could be used for hydrogen generation [10-12]. Steam reforming and aqueous phase reforming (APR) have been attempted previously for hydrogen production from such viscous feedstock [13-15].

APR allows processing of viscous feedstock that cannot be vaporized without decomposition [11]. In APR, substrates are reformed while they are in the liquid phase at higher pressures and lower temperatures than steam reforming. APR has several advantages over steam reforming: 1) It requires less overall energy by saving the latent heat of vaporization; 2) It reforms at substantially lower temperatures and 3) It harnesses the full potential of the water gas shift reaction, which is thermodynamically inhibited at steam reforming temperatures [16-19]. However, a recent review done on the APR process by the Pacific Northwest National Laboratory concluded that the activity (the conversion rate of the feedstock) is too slow to be economically viable (reactivity within the Weiss Window $<1x10^{-06}$gmol glycerol converted/cc-sec in a 1300 hours test, with 10% glycerol feed and a precious metal catalyst) [20]. Slow APR hydrogen production rates occur mainly due to diffusion resistance [21] causing low molar fluxes per unit volume (number of molecules converging to the catalytic surface) around the solid (catalyst) layer [20]. This causes more substrate molecules to exit the reformer without reacting at the catalyst surfaces [22].

Although APR possesses several key advantages over steam reforming, the process displays several major drawbacks too. Viscous feed liquids like glycerol has transport limitations on the catalytic surface. Transport limitations can occur due to several reasons like increased particle size, and lower metal loading on the catalyst [23, 24].

Steam reforming, on the other hand, is performed in the vapor phase and has historically resulted in high hydrogen yields using short-chain hydrocarbons [4, 13]. Steam reforming oleo chemicals and their derivatives are challenging due to heat and mass transfer limitations associated with changing the state from a viscous liquid (droplets > 100 nm) to a gas (particles < 1 nm) [25-28]. In fact, studies have concluded that conventional steam reforming is ineffective energetically for reforming long chain - highly viscous oxygenated hydrocarbons [9, 11, 14] generated from biobased feedstock.

Both APR and steam reforming are not effective in reforming most bio based feedstock. These limitations lead evaluation of an alternative reforming concept where electrically charged viscous liquid droplets will be reformed when they are between 1-100 nm in diameter, i.e., nanophase reforming. The state of charged nanodroplets at these diameters are neither gas nor vapor [29, 30]. The droplets will have physical properties closer to a liquid [31], but, will behave like a vapor [29, 30]. Due to the charges, they will have the ability to respond to electrostatic forces [32, 33]. Due to the reduced droplet size, the surface area will be larger and the molar flux per unit volume in a droplet converging into the catalyst surface will be orders of

magnitude higher than APR [32-35]. We propose to capitalize on these unique properties of nanodroplets to develop a novel reforming technique that, in principle, will offset the major limitation of APR, slow reaction rates.

The long-term goal of this study is to develop a reforming technique to produce hydrogen mainly from bio renewable feedstock which has markedly different physiochemical properties from petroleum based hydrocarbons. The overall objective of this study is to improve the basic understanding of the chemistries involved in catalytic reforming of positively charged substrate droplets over a grounded metal/carbon-graphite catalyst surface.

The central hypothesis of the study is that reforming electrically charged substrate droplets can significantly increase substrate conversion in comparison to reforming non-charged substrate droplets.

To test the above hypothesis, glycerol, a representative bio-renewable substrate was chosen as the test material. With a worldwide surge in biodiesel production, there is now a glut of glycerol market. Consequently, the price of glycerol has drastically dropped. This glycerol surplus warrants our quest for new uses which will bring added value to this once valuable commodity. Traditional applications of glycerol have been mostly in the pharmaceutical, toothpaste, tobacco, food, urethane and the manufacturing industry. Glycerol has been a primary ingredient in the manufacture of lacquers, varnishes, inks, adhesives, synthetic, plastics, regenerated cellulose and explosives [2].

In order to form charged glycerol droplets, a techniques called as electro-spray was used. Electro-spray technique was first experimented in 1917. Since then it has been developed by great amount[36]. It has been used in various types of applications including high performance liquid chromatography (HPLC), mass spectroscopy [34, 37]. A detailed review of steam reforming, aqueous phase reforming and electro-spray would follow.

1.2 Objectives of the Study

The overall goal of this study is to develop a reforming technique that is amicable to viscous fluids reforming. The specific objectives of this study are to:

1. Understand the effect of infusing an electric charge to liquid phase and gas phase viscous glycerol on H_2, CO, CO_2 and CH_4 selectivity and glycerol conversion,
2. Evaluate the effect of voltage and temperature on H_2, CO, CO_2 and CH_4 selectivity and glycerol conversion.

CHAPTER II

GLYCEROL REFORMING TECHNIQUES

2.1 Glycerol Steam Reforming

Glycerol (1,2,3-propanetriol, $C_3H_8O_3$) is a colorless, odorless, viscous liquid with a sweet taste, derived from natural and petrochemical feedstocks and it is a major by product of biodiesel production process [2]. The name glycerol has been derived from Greek name called "glykys" meaning sweet taste. Glycerol has a specific gravity of 1.261 g/ml and a boiling point of 290 ^{o}C. Glycerol has about 1500 end uses, but is increasingly viewed as a desirable alternative substrate for bio renewable energy generation. One such alternative use of glycerol is as a substrate for hydrogen generation.

Reforming process is the most widely used method to produce hydrogen from oxygenated hydrocarbons. There are four major variations within the reforming processes, namely, steam reforming (SR)[1, 4, 38], auto thermal reforming [39, 40], aqueous phase reforming (APR)[8, 41, 42], and partial oxidation (PO)[1]. Among these, steam reforming is the most commonly used and experimented. Aqueous phase reforming is the most recently developed method. The main differences between the two processes are that steam reforming is carried out at higher temperatures and lower pressures while APR is carried out at lower temperatures and higher pressures.

Ideally, in steam reforming, the oxygenated hydrocarbons and steam are sent over a noble metal catalyst where these substrates are endothermally converted to hydrogen [37] and carbon dioxide. The stoichiometric equation is as follows:

$$C_3H_8O_3 + 3H_2O \rightarrow 3CO_2 + 7H_2 \qquad (\Delta H^o_{298} = +346.4 \text{ kJ/mol}) \qquad (1.1)$$

Thus converting glycerol in to hydrogen from steam reforming is thermodynamically favorable at higher temperature and lower pressure. This is so since the reaction is highly endothermic and the products are gaseous. According to the Le Chatelier-Braun principle, high temperatures and low pressures shifts the equilibrium towards the desired products. However, in practice, this ideal conversion could not be achieved. There are several other products formed simultaneously and the product composition varies depending on the catalyst used. For example, carbon monoxide and methane can be obtained as by products from glycerol reforming [13, 43, 44].

Reactions associated with glycerol catalytic reforming [43, 45] are as follows.

Steam reforming reaction

$$C_3H_8O_3 \xrightarrow{H_2O} 3CO + 4H_2 \qquad (\Delta H = +250 \text{ kJ/mol}) \qquad (1.2)$$

Water-gas shift reaction

$$CO + H_2O \longleftrightarrow CO_2 + H_2 \qquad (\Delta H = -41 \text{ kJ/mol}) \qquad (1.3)$$

Methanation reaction

$$CO + 3H_2 \rightarrow CH_4 + H_2O \qquad ((\Delta H = -206 \text{ kJ/mol}) \qquad (1.4)$$

The overall glycerol reforming reaction can be written as

$$C_3H_8O_3 + 3H_2O \rightarrow 3CO_2 + 7H_2 \qquad (\Delta H = +128 \text{ kJ/mol}) \qquad (1.5)$$

A main sub-reaction that is believed to be occurring during steam reforming is the water-gas shift (WGS) reaction. The reaction is depicted below:

$$CO + H_2O \longleftrightarrow CO_2 + H_2 \qquad (\Delta H = -41 \text{ kJ/mol}) \qquad (1.6)$$

As WGS is an exothermic, the reaction favors low temperatures.

Several studies were reported on glycerol reforming process including our own research group [46, 47]. Hydrogen selectivity of 90 % was reported using Ru/Y_2O_3 catalyst at 600 ^oC[45]. Our research group reported 60 and 70 percent hydrogen selectivity at 900 ^oC with Ni/Al_2O_3 and $Pd/CeO_2/Al_2O_3$ catalysts respectively. However from a regimen of experiments Ni/CeO_2 was found to be the best catalyst for glycerol reforming showing 74 % hydrogen selectivity at 600 ^oC.

2.2 Aqueous Phase Reforming (APR)

Aqueous-phase reforming (APR) is a technique that has been developed to produce hydrogen from oxygenated hydrocarbons such as glycerol, sugars and sugar alcohols. APR is unique in that the reforming is done in the liquid phase. The process generates hydrogen without volatilizing water, which represents major energy savings. Furthermore, it occurs at temperatures and pressures where the water-gas shift reaction is favorable, making it possible to generate hydrogen with low amounts of CO in a single chemical reactor. In the same time, APR has higher probability to produce water (H_2O) with lower temperatures. By taking place at low temperatures, the process also minimizes undesirable decomposition reactions typically encountered when oxygenated hydrocarbons are heated to elevated temperatures. In the same way,

the reactor and catalysts can be altered to allow generation of high-energy hydrocarbons (propane, butane) from biomass-derived compounds

A multiplicity of technologies, accomplish the separation of carbohydrates from biomass, and the appropriateness of a feedstock for this process (APR) depends on determining the proper separation technology. Some feed stocks are already aqueous carbohydrate streams. Unlike other hydrogen-producing technologies, APR requires no non-renewable resources and is emissions neutral. Unlike steam reforming processes, APR produces hydrogen from liquid-phase solutions, resulting in considerable energy savings.

For example, when ethylene glycol was reformed at 225 ^{o}C and 2510 kPa pressure on Ni/Sn catalyst, a hydrogen selectivity of 90 % with reduced amount of CO production was reported [41]. Another study showed for glycerol 75 % hydrogen selectivity with 225 ^{o}C and 29 bar pressure on Pt/Al_2O_3 catalyst [48]. However, only a few studies have been reported on aqueous phase reforming and, as a result, only limited data are available [5, 6, 41, 49, 50].

2.3 Electro-Spray

Large substrate particle size is a limiting factor on the mass transfer phenomena on a catalyst bed. This is more critical when it comes to viscous liquid reforming. A workable solution to this is atomizing substrates into finer particles and introducing this liquid cloud onto the catalyst bed. Fluid atomization can be achieved by mechanical means or by applying high voltage to split the liquid feed. Rupturing a

liquid feed into finer droplets using high voltage is called as “Electro-spraying”. Electro-spray is a technique mostly used in physical chemistry. From the literature the early electro-spray experiments were performed during 1917’s [36]. This technique is still used in chromatography and it is selected as the mode of atomization for several reasons:

1. Electro-spray has been proven feasible to atomize glycerol in previous studies[51-54].
2. The substrate spray could be appropriately charged – it is hypothesized that by charging the catalyst surface with an opposite charge, the glycerol droplets could be forced towards the catalyst surface as opposed to a Brownian motion-random walk type process.
3. It has been proven that the resultant particle size is dependent on applied voltage, substrate viscosity, distance between the electrodes and the capillary diameter. It is projected that the substrate particle diameter could be controlled due to these dependencies thereby facilitating future reforming studies.

Electro-spraying is a technique used to atomize a liquid stream by means of electrical forces. Here, the liquid is subjected to high electrical potential while it travels through a capillary tube. The electric field forces the liquid to disperse into fine droplets when it comes out from the capillary column. In the following section, the electro-spray technique is discussed. Sub-section 2.3.1 discusses various types of electro-sprays while 2.3.2 elaborates on various applications of electro-sprays.

Section 2.3.3 concludes the section with the applicability to the glycerol reforming process.

2.3.1 Electro-spray modes and techniques

There are several different modes of electro-spraying. These modes are basically categorized according to the physical appearance of the liquid jet and the size of the droplets that ejects from the capillary column. The size of electro droplets range from hundreds of micrometers to tenths of nanometers [55]. The basic different modes of electro-spraying are as follows:

1. Dripping modes
2. Jet modes

Dripping mode:

Electro-spraying happens when the liquid flow through the capillary is sufficiently small so that drops detach individually from the tip of the capillary column. At this time, application of a high electrical potential to the incoming liquid flow increases the dripping frequency as well as reduces the droplet size [56].

This dripping can be further classified as dripping mode, microdripping mode and spindle or multi spindle mode [55]. Figure 2.1 shows pictures of typical formation of electro-spray via dripping mode. When the high electrical field reaches its critical value dripping mode turns in to the jet mode.

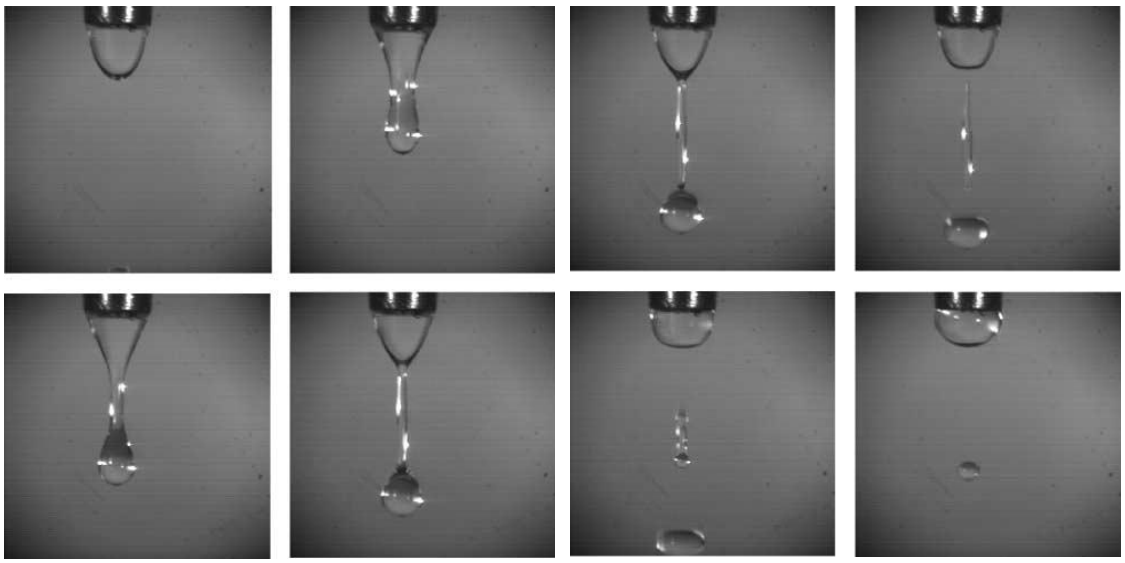

Figure 2.1 Dripping modes[56]

Jet mode:

Best atomization can be achieved in the jet mode. Here, liquid through the capillary breaks up in to droplets due to two instabilities, namely varicose and kink instabilities [56]. Jet mode can be further classified in to sub-modes namely cone jet, oscillating jet, multi jet and precession mode [55]. Most important mode for electro-spraying applications is cone jet mode [37, 52, 55, 57, 58]. In this mode, meniscus of the liquid coming out from the capillary is assumed to be in a regular cone shape with a length of jet less than 1000 micrometers. Figure 2.2 illustrates formation of all the modes discussed above.

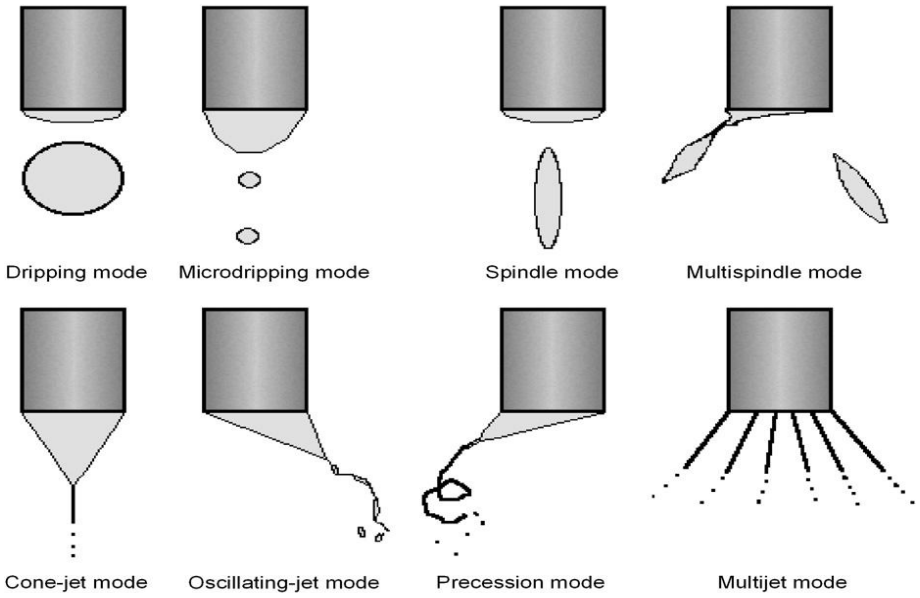

Figure 2.2 Various modes of electro-spraying[55]

2.3.2 Application of electro-spray

There are many different applications in electro-spraying. Pharmaceutical industry, electronic industry, food industry, paints and mostly in laboratory equipments uses electro-spraying in various forms. Electro-spraying is widely used in thin film applications in electronic industry where thickness of the film is less than 10 micrometers - such as solar cells, fuel cells, lithium batteries. Fine particle applications on ceramic coatings, paints and in emulsions also uses of electro-spray technology. An important application of electro-spraying is in chromatography. Electro-spray is used in chromatography to have better separation of ions.

2.3.3 Electro-sprays on reforming process

There has been much work done on using electro-spray techniques for viscous liquids atomization. However, this technique has never been attempted in reforming. When it comes to aqueous phase reforming of viscous liquids, feed flow atomization is important to overcome the transport limitations that occur in the catalytic surface. As electro-spray technique has a higher capability to generate fine/uniform droplets that could be electrically charged, this technology is best suited for the purpose of understanding the effects of the substrate phase (liquid/solid) and charge (charged/uncharged) on the propensity to produce hydrogen than mechanical atomization.

Many references can be found on electro-spraying of glycerol as well as other viscous liquids [54, 57-62]. Glycerol electro-spray has been investigated and found that it shows nano regime spray with very small flow rates(0.35 nl/s) and with high voltage(3-4 kV)[59]. Same study suggests that lower current through the high voltage generator resulted in finer particle sizes.

It has been reported that the performance of the spray depends on several factors. Viscous forces, drag forces, liquid flow, strength of the electric field and as well as the corona discharge affects the particle size distribution. It has been shown that increasing voltage resulted in finer droplets [62]. Corona discharge phenomena haven't been studied well enough to explain the theory of discharging. There are several studies that has been carried out to determine the effect of corona discharge on the performance/formation of electro-spray [63, 64]. A limitation during a set of

such experiments was the inability to obtain satisfactory spray due to corona discharging. Placement of a secondary opposite charge ring before the tip of the capillary column [63], were reported to ameliorate the discharging issues.

CHAPTER III

MATERIALS AND METHODS

This chapter discusses the materials used and the methodology followed in Electro-spray reforming. Section 3.1 presents the materials used while 3.2 describes the Instrumentation used in forming the electro-spray. Section 3.3 depicts all the equipments used for the reforming experiment. Finally section 3.4 describes the methodology followed in this electro-spray reforming process.

3.1 Reagents and Materials

Purified glycerol was purchased from Sigma Aldrich (St. Louis, Mo, USA)**.** For the catalyst preparation, the precursors cerium nitrate hexahydrate [$Ce(NO_3)_3.6H_2O$] and nickel nitrate hexahydrate [$Ni(NO_3)_2.6H_2O$] were purchased from Sigma-Aldrich (St. Louis, Mo, USA). The supported base material, activated carbon, was purchased from Calgon Carbon Corporation (Pittsburg, Penn, USA). The makeup inert gas used was nitrogen [N_2] (Ultra high purity N_2, Airgas Columbus, Miss, USA)

3.2 Electro-Spray Instrument

Nanoscale spray of glycerol/water was obtained with a high voltage device from Glassman High Voltage Incorporated (FC-30R4, High Bridge, NJ, USA) which had the capacity up to 30,000 kV of high voltage. The liquid feed was fed with a high pressure liquid chromatography (HPLC) pump (LC-20AT, Shimadzu Scientific Instruments, Columbia, Md, USA).

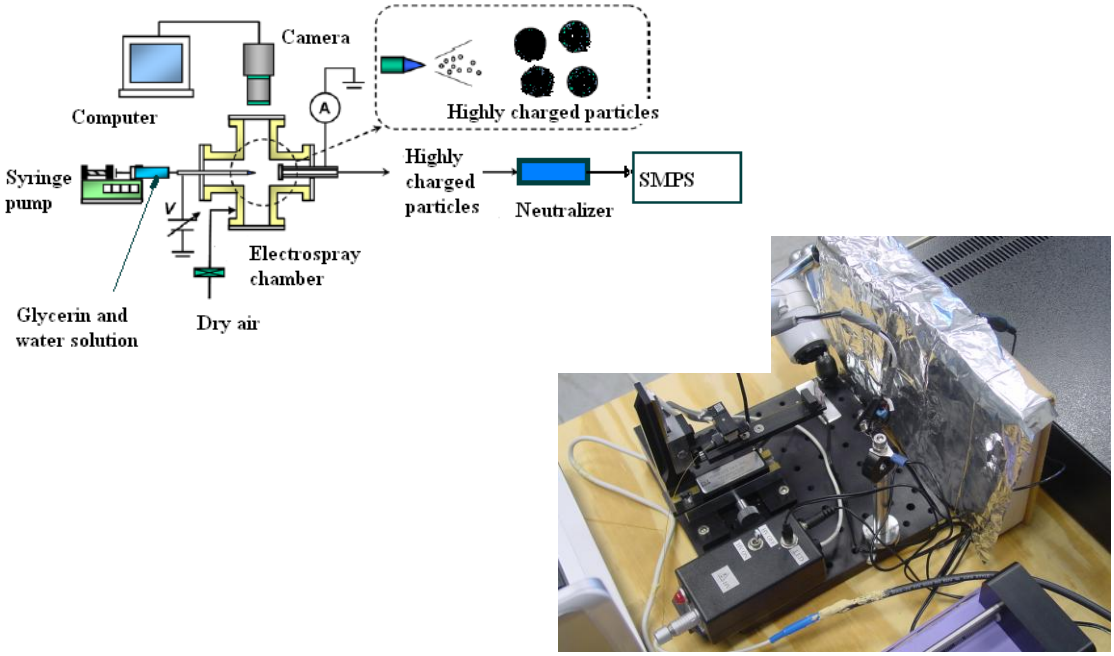

Figure 3.1 An electro-spray schematic and system setup for production of glycerol nanodroplets during preliminary studies

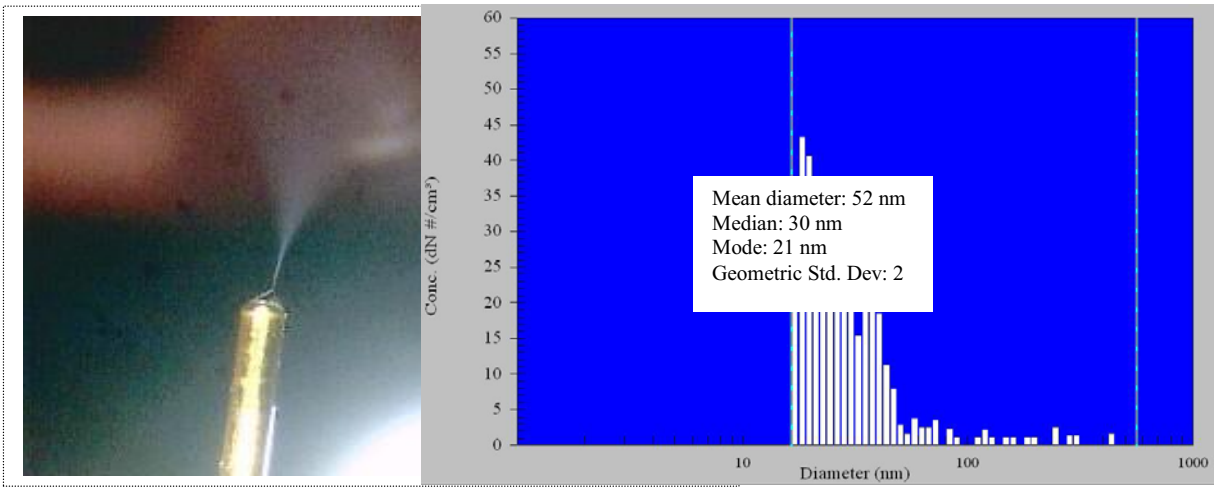

Figure 3.2 Cloud of glycerol nanoparticles produced by the electro-spray technique captured with high resolution imaging (Left) and Particle size distribution of glycerol nanospray (Right)

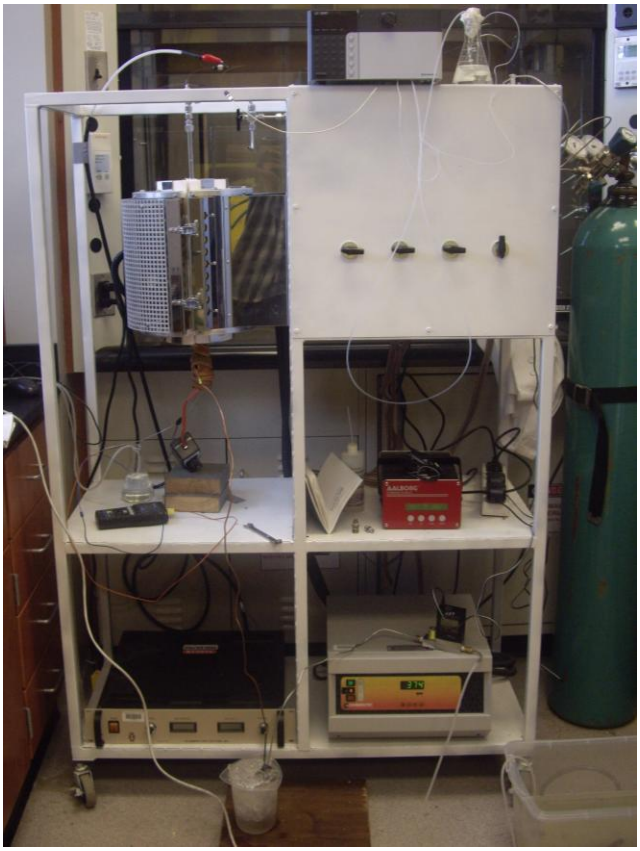

Figure 3.3 Electro-spray unit retrofitted to the reformer

The tubing used for liquid flow was a silicon-coated capillary with an internal diameter of 50μm (Polymicro Technologies Phoenix, Ariz, USA). The nanoscale spray formation was monitored using a high resolution microscope by Bodelin Technologies (Proscope HR, Lake Oswego, Orig, USA). It should be noted that conditions for nanospray formation using glycerol/water mixtures were identified as a part of a separate project. More information on glycerol nanospray formation could be found elsewhere[65]. Figure 3.2 shows a high resolution photograph and the distribution of nano-particles on glycerol electro-spray generation experiment carried out previously by our research group. The electro-spray formation devise and the unit retrofitted into the reformer are presented in Figures 3.1 and 3.3 respectively.

3.3 Reforming Instrument

The reforming setup was designed and developed in the Mississippi State Agricultural and Biological Engineering Department shop. All the fittings were purchased from Swagelok Company (Solon, Ohio, USA). Thermal reactor (tube furnace) was purchased from Carbolite Limited (VTS-12/200, London, UK). Gas flow controllers were purchased from Cole Parmer Instrument Company (K-32907-59, Vernon Hills, Illinois, USA). Finally, the reformed gas was analyzed by a gas chromatograph unit coupled with duel thermal conductivity (TCD) and flame ionization detectors (FID) from Agilent Technologies Inc. (GC6890, Palo Alto, Calif, USA).

3.4 Methodology

This study was consisted of two experiments. The goal of the first experiment was primarily to determine whether there was an effect of charge on the reforming performance of sprayed glycerol droplets and, if so, determine the optimal temperature where the product selectivities were maximum. The goal of the second experiment was to observe the effect of high voltage on the reforming performance of electrically charged glycerol droplets. During the entire course of the experiments, identical catalysts and glycerol/water mixtures were used. Both experiments were carried out with 3 replicates per experiment.

3.4.1 Catalyst Preparation

Catalyst selection was based on a successful previous study performed on glycerol steam reforming. These studies identified Ni/CeO_2 to be the best catalyst for the glycerol reforming [46, 47].

However, the catalyst support CeO_2 used in the aforementioned study was non-conductive. The present experiment warranted a conductive support. Consequently, carbon was used as the support in this study. Catalyst preparation was done by step impregnation [45]. Loadings of Ni and CeO2 were 10 % and 5 % by weight respectively. Finally, the prepared catalysts were calcined at 500 ^{o}C for 8 h in N_2. The prepared Ni/Ce/C catalyst was then dried in an incubator prior to use.

3.4.2 Experiment I

For experiment one, six temperatures were chosen so that the boiling point of glycerol (290 ^{o}C or 554 ^{o}F) fell within the range. The temperatures chosen were: 250, 275, 300, 325, 350, 400 ^{o}C. This temperature range was chosen in order to study to reforming of glycerol in the liquid phase as well as gas phase. At temperatures below 300 ^{o}C the substrate glycerol could be considered to be in liquid phase (droplets) whereas at temperatures above boiling point, the droplets would be predominantly vaporized and be in gas phase (as the boiling point of glycerol is 290 ^{o}C). At these temperatures both phases exist at atmospheric pressure. This will provide new information since liquid phase reforming is normally undertaken with high pressure systems [6, 66].

In this experiment, a voltage of 6000 V was initially applied to the feed glycerol. This voltage was chosen because: 1) it was determined from previous experiments that glycerol successfully atomizes to a particle size distribution having a median diameter of approximately 30 nm at this voltage and 2) this is the mid-point of the voltage range that the manufacturer recommended for the electro-spray unit. The liquid stream was positively charged while the conductive carbon catalyst was negatively charged (grounded). At this voltage when steady state conditions prevailed, GC data was recorded. The experiment was then repeated without applying a voltage across the liquid stream and the conductive catalyst.

The glycerol/water flow rate fixed at 0.004 ml/min. In preliminary studies this flow rate produced best spray pattern for electro-spraying [55]. Also, since it was

necessary to select a region where the flow rate was not too low to garner 100% conversion (for comparison purposes) or too high to wet the catalyst surface this flow rate was chosen.

The feed glycerol/water mixture molar ratio was selected to be 1:3 as this is the stoichiometric ratio needed for a complete reaction. All the experiments were carried out with a gas hourly space velocity ($G_{Glycerol}HSV$) of 0.35 ml/g-cat/h. The makeup gas flow of 20 ml/min of N_2 was used.

3.4.3 Experiment II

As described earlier, the goal of this phase was to understand the effects of varying voltage on the performance of reforming charged glycerol droplets (liquid and vapor phase). During this phase, same parameters, i.e., flow rate, pressure (atmospheric), glycerol/water molar ratios, were applied except for the varying voltages. As the intention was to compare effect of applied voltage on the efficacy of reforming, six voltages were chosen. The selected voltages were: 0, 2000, 4000, 6000, 8000, 10000 V. During the first part of the experiment, a reforming temperature of 350 ^{o}C was selected. The temperature was selected as a result of the results obtained from the first phase (It was apparent that the highest hydrogen selectivity was obtained at this temperature.).

A closer view of the actual reforming set-up (capillary arrangement over the catalyst bed) is pictured in figure 3.4. The capillary was held 5 mm above the catalyst bed surface. Average catalyst bed height was 27.4 mm. Quartz wool was used to

secure the catalyst bed towards the middle of the quarts reactor tube. A thermocouple (Digi-Sense, K type thermocouple) was inserted from the bottom of the reactor to detect temperature variation at the catalyst bed. Figure 3.5 shows a schematic diagram of the experimental setup. The negative lead of the high voltage device was fixed to the thermocouple which touched the carbon-based catalyst bed. This is the experimental setup designed to investigate the effect of electro-spraying on aqueous phase reforming as well as steam reforming. This experiment was conducted as a split-plot design. All of the statistical analysis was undertaken using S-A-S version 9.1. Appendix A details the analysis of variance of this study as well as all the statistical analysis carried out.

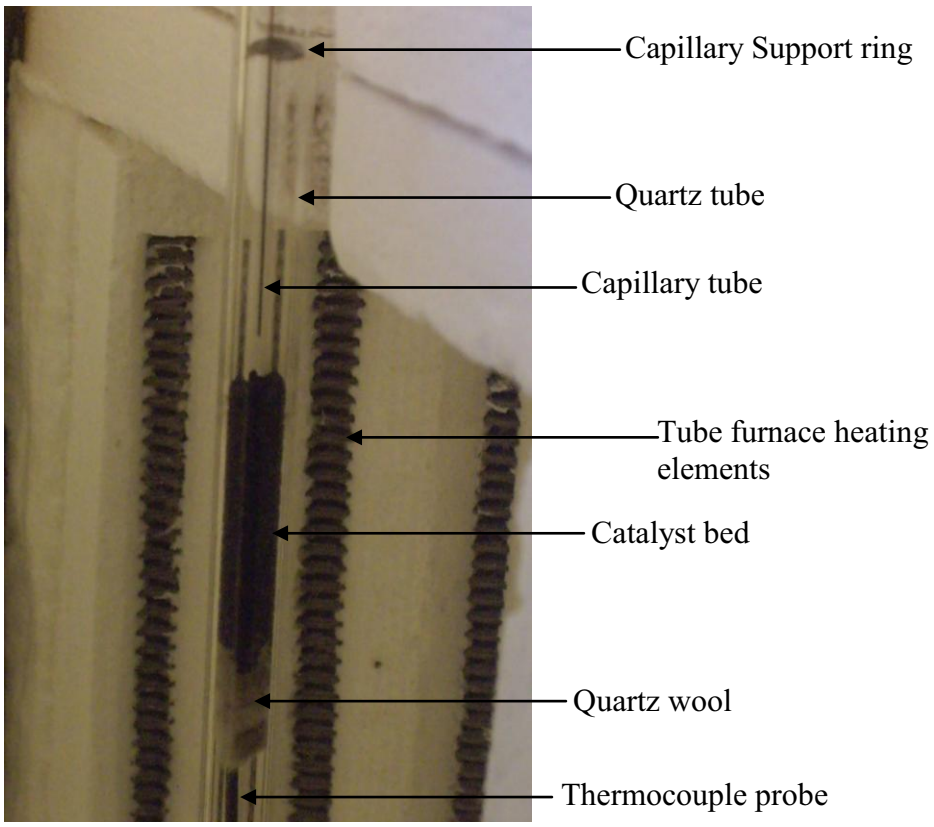

Figure 3.4 A close-up view of the reactor arrangement

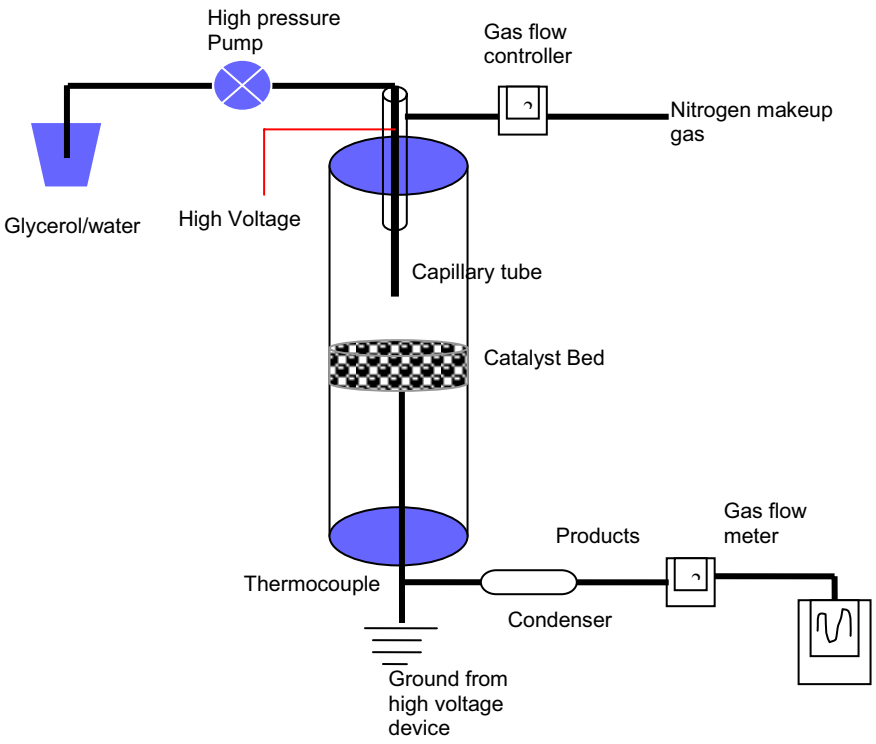

Figure 3.5 Schematic of glycerol reforming system

CHAPTER IV

RESULTS AND DISCUSSION

In this chapter results and findings of the study are presented and discussed. Section 4.1 discusses the results from the first experiment. Section 4.2 discusses the second experiment. Lastly conclusions and recommendations based on the observations are forwarded in section 4.3.

4.1 Electro-Spray Formation

Although not quantified during this study, the formation of the electro-spray jet was clearly seen with the microscope. Figure 4.1 vaguely shows formation of a single large liquid drop when a voltage is not applied across the capillary and the grounded catalyst bed. This mode is called dripping mode [55].

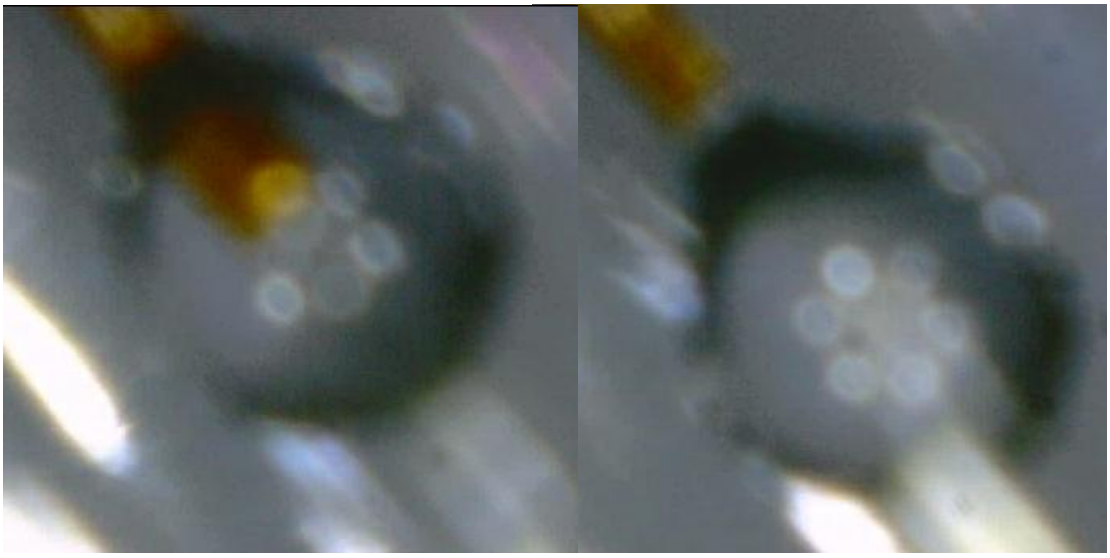

Figure 4.1 Dripping mode of glycerol without an applied voltage

When a voltage (6 kV) was applied to the system, the liquid flow pattern drastically changed and comes to a stable flow with a clearly visible jet spray. Setting the flow to the cone jet spray mode is achieved through a series of fine tuning adjustments of flow rate and voltage. Figure 4.2 illustrates formation of the cone jet mode. It should be noted that readers may not be able to readily visualize the spray since the magnification of the in-line microscope was not high enough. The typical spray size distribution of glycerol electro-sprays have been confirmed to be between 10-100 nm range [55, 65].

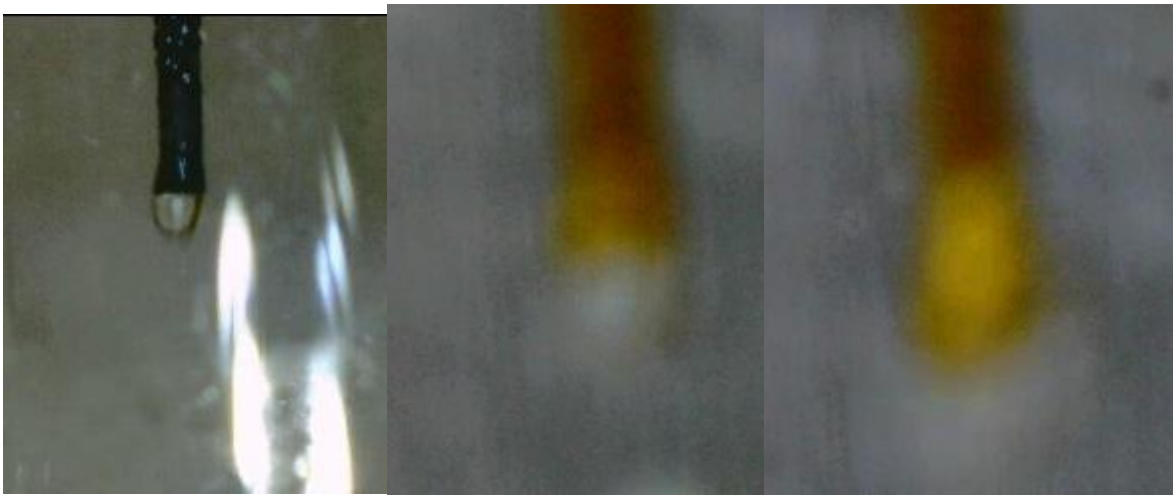

Figure 4.2 Cone jet spray formation of glycerol feed with high voltage

4.2 Effect of High Voltage on Glycerol Reforming

The main goal of this phase of the study was to examine the effect of applied voltage on catalytic reforming of glycerol, an oxygenated hydrocarbon. Here the reforming conditions were maintained similar to that of aqueous phase reforming (APR) with the exception of the pressure. As the pressure inside the reactor was atmospheric, reforming capability was expected to be low compared to APR. The experiment was structured to analyze the four major gaseous compounds produced from the reforming process. It is well known that major gases formed as a result of oxygenated hydrocarbon reforming are hydrogen (H_2), carbon dioxide (CO_2), carbon monoxide (CO), methane (CH_4) [23, 24, 41, 46, 67, 68].

Statistical analysis of the results was carried out according to a split plot experimental design. Least Significant Difference was applied to determine the significance of temperature and the high voltage applied. Three data sets from 3

replicates were analyzed in this statistical analysis. All the comparisons were made at 5% significance level.

4.2.1 Gas yield comparison

One of the most common comparisons in gaseous products analysis is yield. This is a kind of crude measure of reforming performance, but one that still brings a clear comparison of reforming performance high voltage application in the reforming of glycerol. The gas yields were measured directly from the GC analyzer.

4.2.1.1 Effect of substrate charge on hydrogen yield

Hydrogen was the main targeted product from glycerol reforming. Figure 4.3 illustrates trends in the hydrogen yield when a voltage is applied/discharge with varying temperatures. It is clear that at each temperature the yield of hydrogen gas increased with the application of a high voltage except 400 ^{o}C.

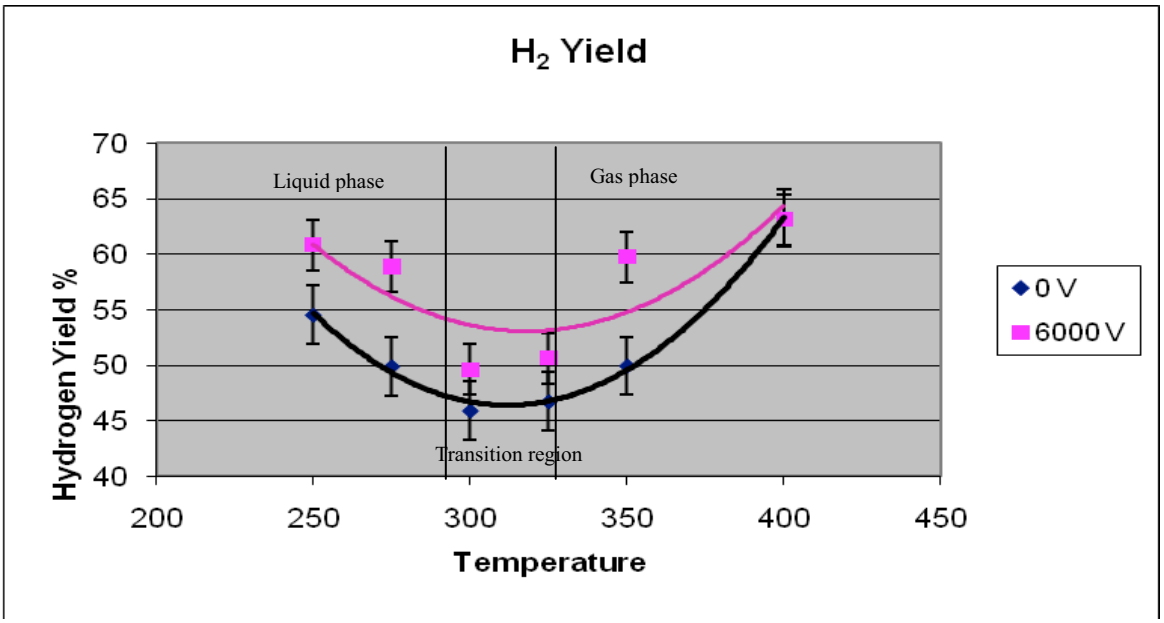

Figure 4.3 Effect of electrical charge and temperature on H_2 yield

With the Ni-Ce/C catalyst and the temperature range tested, hydrogen yield hit a maximum of 63% at 400 ^{o}C. Percentage H_2 yield increase of 19.6% between charged and uncharged reforming was highest at 350 ^{o}C. Results indicate that when the reforming process nears gas phase, the effect of high voltage (the difference between H_2 yield of charged and uncharged glycerol streams) markedly diminishes. It could be presumed that as temperature increases, the feed flow is occupied predominantly with gas phase reactants (comprised of Angstrom sized molecules) where gas-phase reforming chemistry takes place. In contrast, as it was hypothesized, below and near glycerol boiling points, a significant increase of hydrogen yield is observed when glycerol liquid droplets are charged as opposed to non-charged liquid phase glycerol reforming.

It should be noted that regardless of the phase (gas/liquid) the amount of electrical charges exerted to the liquid stream per unit time is constant. Consequently, the number of surface charges per agglomerated droplet will be higher in nano-droplets than gas phase reactants. So, nanodroplets are expected to be attracted more forcefully towards the catalyst than gas phase reactants. The latter principally encounter the catalyst surface as a result of random walk / Brownean motion type process. This premise is further established due to the fact that charged gas-phase reactants result in a higher H_2 yields than their uncharged counterparts at higher than glycerol boiling point temperatures where gas-phase reforming predominantly takes place.

The reduction of H_2 yield at and around the boiling point of glycerol could be attributed to the expense of system energy as latent heat of vaporization. The net reduction of available energy to overcome the activation energy barrier translates into a reduction of hydrogen yield from reforming.

4.2.1.2 Effect of substrate charges on carbon monoxide yield

One of the major products other than H_2 produced during the reforming process is carbon monoxide (CO). As a result of the water gas-shift reaction, CO is consumed to produce H_2 and CO_2. Figure 4.4 shows the CO yield with respect to temperature. It is clearly visible that at higher temperatures (above 350^{o}C) where an increased H_2 yield was observed, CO yield decreased. Although lower temperatures

thermodynamically favor CO conversion to H_2, the kinetics are unfavorable. This may be the reason for low CO conversion to CO_2 at the low temperatures.

However, it is interesting to note that at 275 ^oC where predominantly aqueous phase reforming is expected to occur, an increase of 45.5 % of CO was obtained when the substrate is electrically charged as opposed to reforming uncharged glycerol droplets. This indicates that the primary reforming reaction of glycerol conversion to CO takes place more effusively when the substrates are charged. At 400^oC CO yield of charged reformate has dropped 12% below its uncharged counterpart suggesting even more favorable kinetics. This trend suggests a two-way interaction of electrical charges as well as kinetics favoring glycerol reforming at moderately high temperatures.

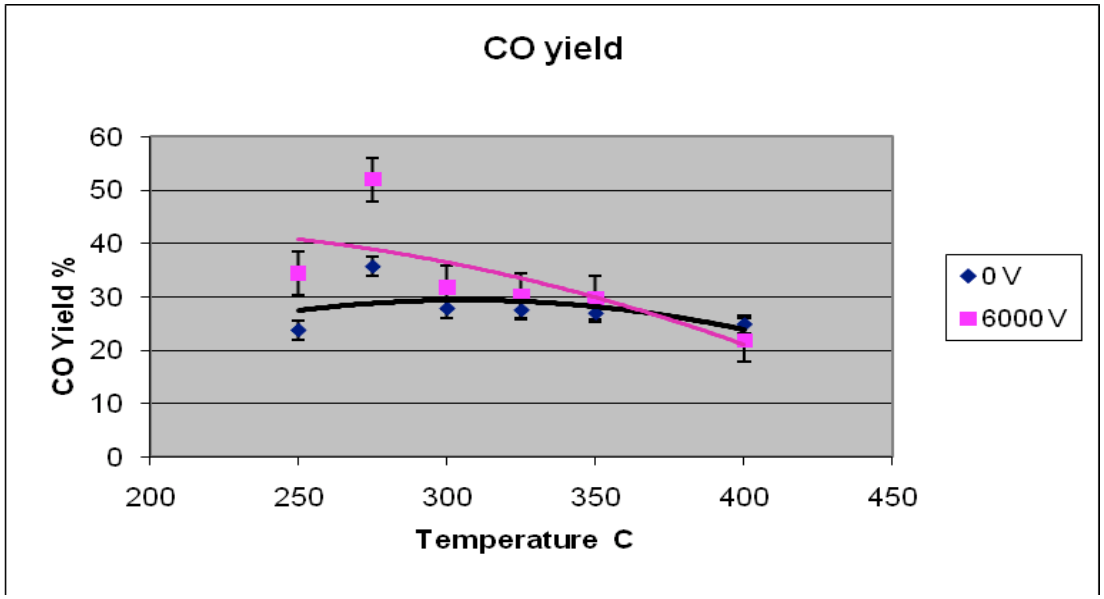

Figure 4.4 Effect of electrical charge and temperature on CO yields

4.2.1.3 Effect of substrate charges on carbon dioxide yield

Carbon dioxide (CO_2) was the expected final product of reforming other than H_2. CO_2 yield surprisingly had smaller change much with the increased temperature. The yield levels stayed lower numbered throughout the experiment. Nonetheless, an applied voltage increased the CO_2 yield in comparison to reforming uncharged substrates. Figure 4.5 depicts the CO_2 yield comparison with charge and temperature conditions.

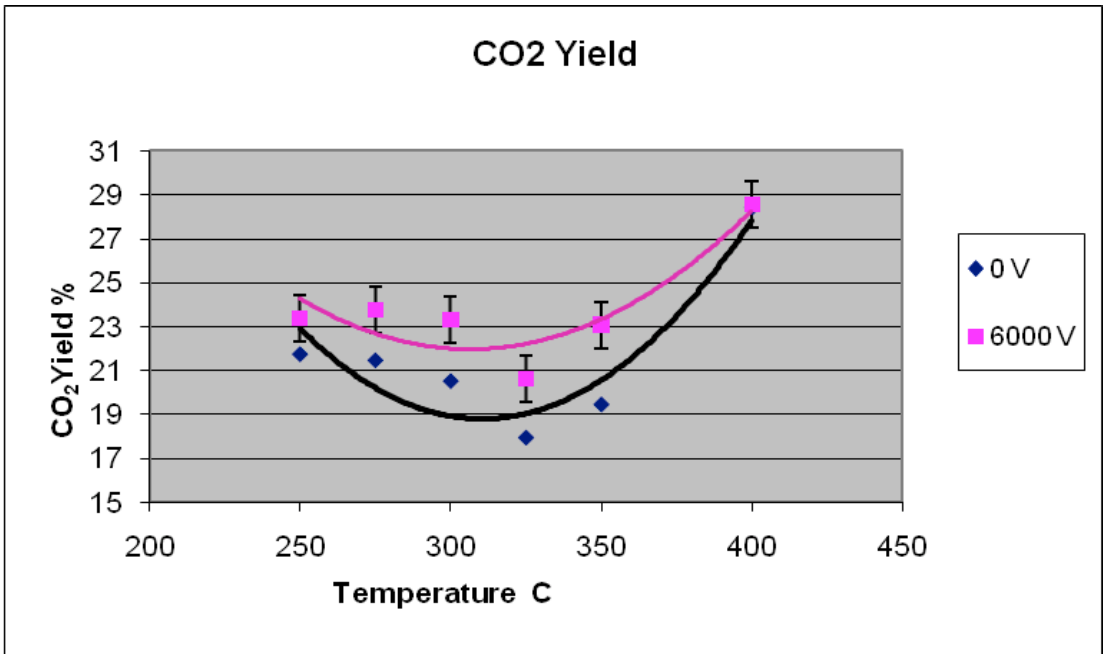

Figure 4.5 Effect of electrical charge and temperature on CO_2 yields

As shown in figure 4.5 CO_2 yield initially being different between charged and uncharged substrate reforming, approached a similar value at gas phase reforming temperatures. This observation again reinforces the observation made earlier that the effect of electrical charges dominates at liquid phase reforming and diminishes at gas phase reforming temperatures.

4.2.1.4 Effect of substrate charges on methane yield

Methane is an undesirable by-product of glycerol reforming. Methane is produced by the methanation reaction that occurs on the catalyst bed. Methanation is favored at low temperatures and lower pressures. In this experiment, we observed an increase in methane production with an applied voltage. This can be attributed to high overall reaction rates due to enhanced mass transfer resulting in an increase of even undesirable reactions. In fact, this observation is in total agreement with catalysis science where a catalyst not only increases the rate of forward reaction but also the reserve reaction and all associated reactions. However, in general the methane yield remained low. Figure 4.6 illustrates the methane yield distribution with temperature and applied voltage. Here also the same behavior is observed - with the increase in temperature, applying a voltage seems not to have a significant effect on CH_4.

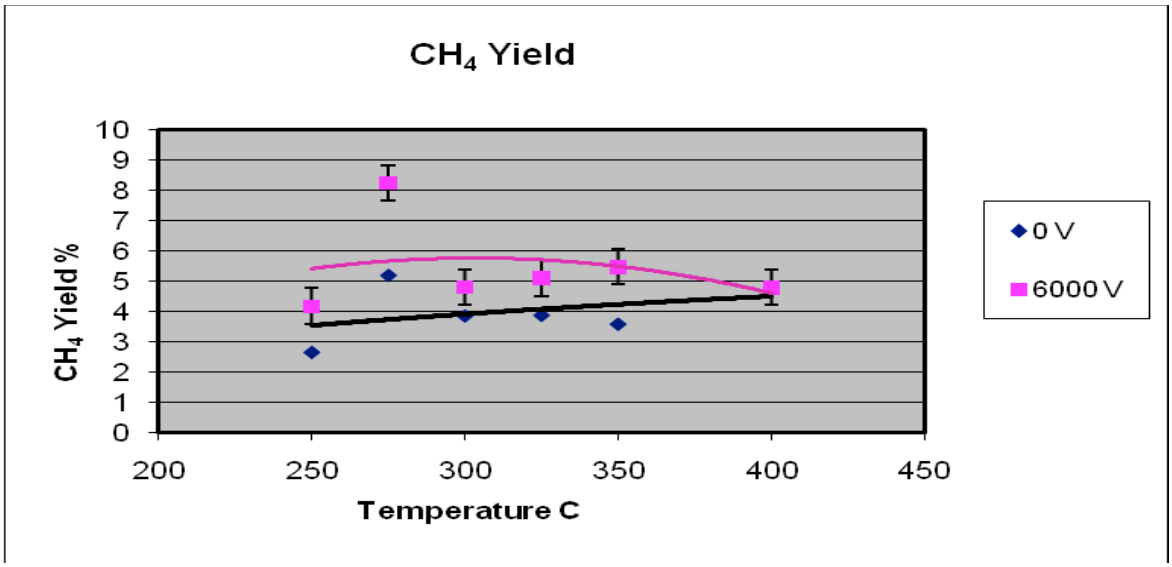

Figure 4.6 Effect of electrical charge and temperature on methane yields

4.2.2 Effect of electrical charge and temperature on product selectivity

Selectivity is a much precise form of presenting the performance of a reforming reaction. In this reaction, selectivity of a given product was calculated as follows:

$$Hydrogen\ \ Selectivity(\%) = \frac{H_2 moles\ \ produced}{Theoritical\ \ H_2 moles\ \ produced} \times 100$$

$$Selectivity\ \ of\ \ i\ \ (\%) = \frac{C\ \ atoms\ \ in\ \ species\ \ i}{C\ \ atoms\ \ produced\ \ in\ \ gas\ \ phase} \times 100$$

Where, *i* is a selected gaseous product. We have concentrated on only three gaseous products other than hydrogen. However, it should be noted that in reality, there may

be more than three gaseous products in the product spectrum. Therefore, the calculations contain some inevitable error.

4.2.2.1 Effect of electrical charge and temperature on hydrogen selectivity

The effect of electrical charge and temperature on hydrogen selectivity is shown in Figure 4.7. It should be noted that hydrogen selectivity reached a maximum of 62 % when a voltage was applied at a temperature of 400 ^{o}C. A minimum selectivity of 40% was observed with an applied voltage at 300 ^{o}C which was closer to the glycerol boiling point. Surprisingly, lower temperatures showed comparatively higher selectivities than 300 ^{o}C. This can be explained as it was done earlier with transition theory.

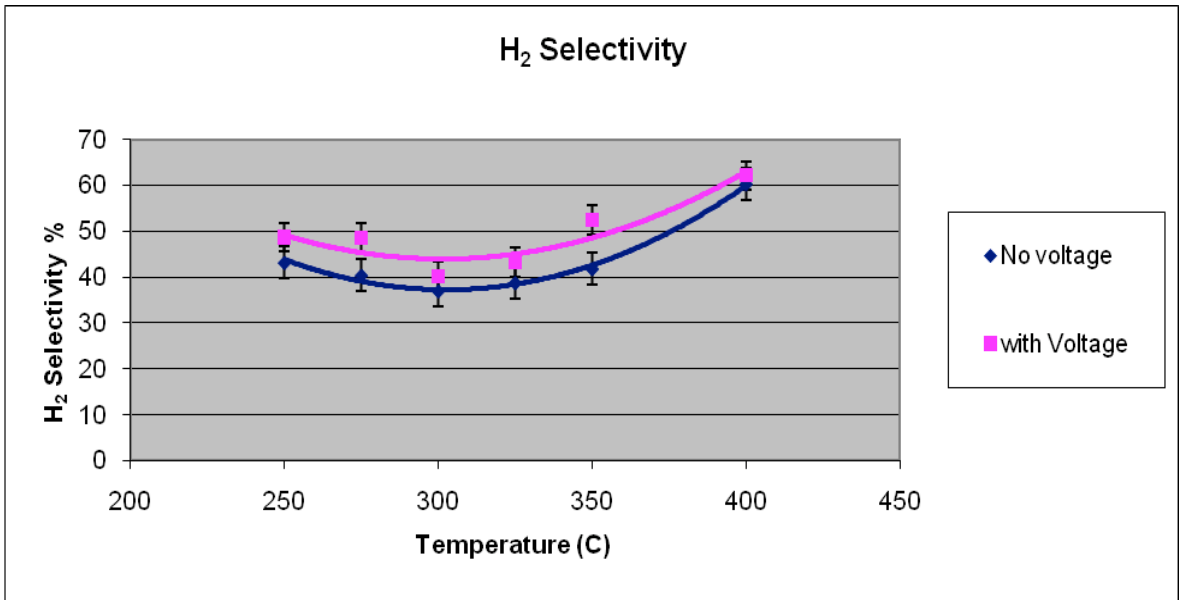

Figure 4.7 Effect of electrical charge and temperature on H_2 selectivity

Table 4.1 H_2 selectivity data with/without voltage

Temperature	H_2 Selectivity	
	Without Voltage	With Voltage
250	43.13	48.63
275	40.36	48.57
300	36.96	40.24
325	38.77	43.19
350	41.81	52.42
400	60.19	62.04

As with H_2 yields, a similar pattern can be observed here as well as temperature increased, the gap between the H_2 selectivities of charged and uncharged reformate was reduced. When gas phase reforming temperatures are approached, the difference between the two reforming approaches becomes negligible. Actual selectivity values are presented in Table 4.1. The statistical analysis suggested a quadratic trend for the hydrogen selectivity. The pattern of variation of hydrogen selectivity with reaction temperature is discontinuous during the transition period and this is clearly visible in figure 4.8.

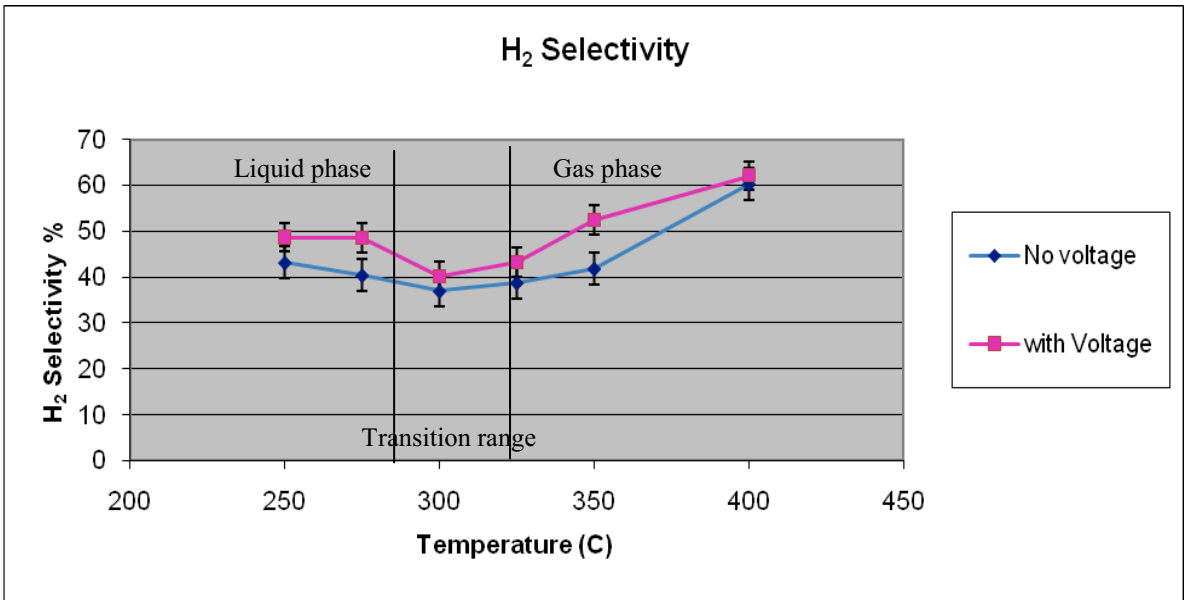

Figure 4.8 Raw data depicting hydrogen selectivity

As can be seen in figure 4.8, the drop in selectivity is initiated around 300 ^{o}C and continues to 325 ^{o}C. This range is much wider than the boiling point of glycerol and should be taken into account when designing reformers.

Increase in hydrogen selectivity is a good measure to determine the effectiveness of charged vs uncharged substrates on reforming. Figure 4.9 shows the increase in hydrogen selectivity between charged and non-charged substrates with temperature. A maximum increase of 10.6 was reported at 350 ^{o}C. This is a 25 % increase in selectivity than reforming non-charged glycerol droplets at same temperature.

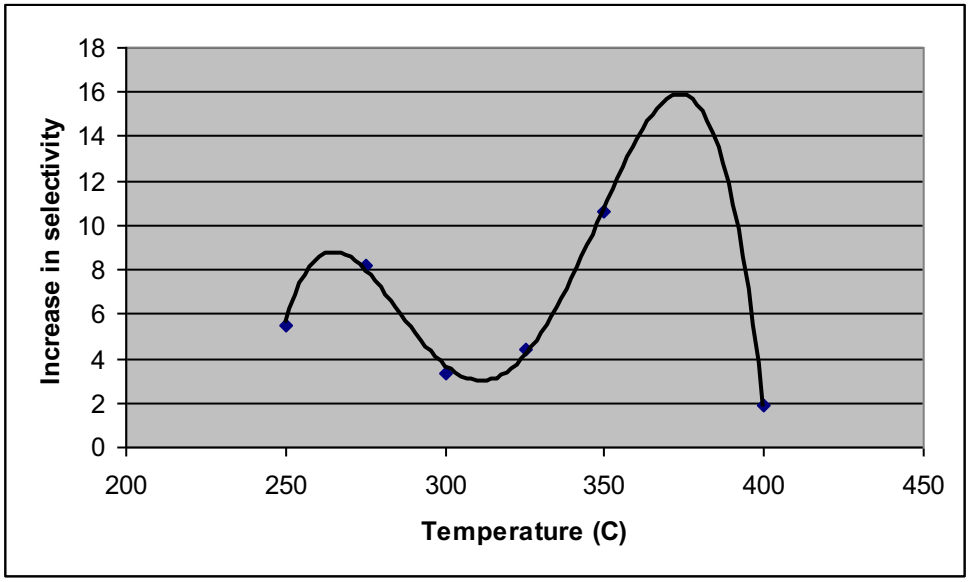

Figure 4.9 Increase in hydrogen selectivity between charged and non-charged substrate reforming

Figure 4.9 illustrates how application of an electric charge (high voltage) affects H_2 selectivity. Here, three major points could be pointed out: 1) A sudden reduction in increase of selectivity is apparent during the transition interval between liquid phase glycerol and gas phase reforming; 2) There are optimum temperatures where hydrogen selectivity is maximum in aqueous phase charged particle reforming and gas phase charged particle reforming; 3) When temperature is increased beyond a certain point (> 375 ^{o}C), the effect of having a charge on the (gas phase) substrate becomes less evident.

A percentagewise demonstration would be an even a better indicator to illustrate this behavior. Figure 4.10 shows the percent increase of hydrogen selectivity of charged substrate reforming as opposed to a substrate without an applied voltage.

The percentage increase was always above 10 % with the exception at 300 ^{o}C where the latent heat of vaporization interferes with the activation energy barrier. At 400 ^{o}C, the percent increase drastically drops to 3 % where gas phase reforming occurs. This suggests that a nanospray of substrate significantly increase the performance of liquid phase reforming process while has a negligible effect on gas phase reforming.

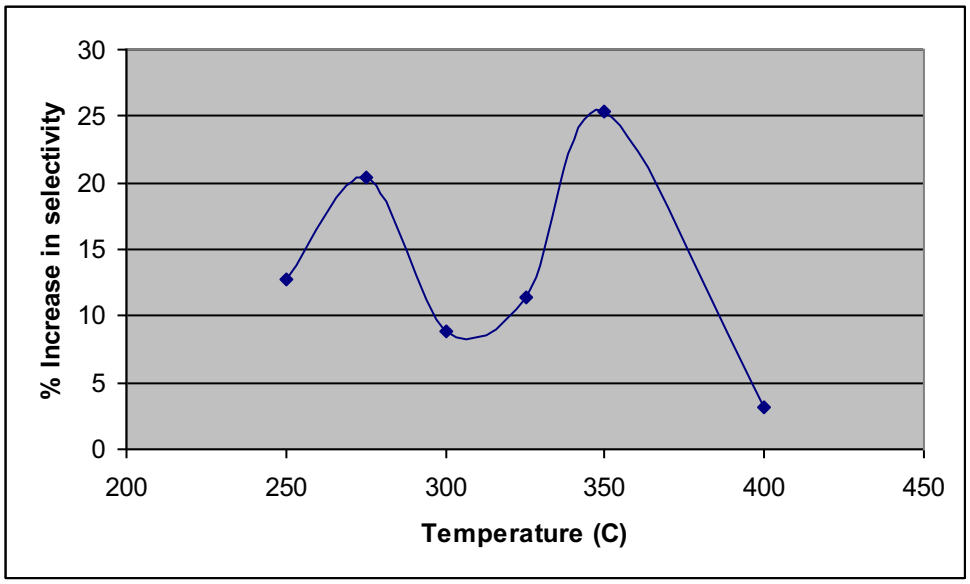

Figure 4.10 Percentage increase in hydrogen selectivity of charged vs uncharged glycerol reforming

4.2.2.2 Effect of electrical charge and temperature on carbon monoxide selectivity

Carbon monoxide is an undesired by product of glycerol reforming. The amount of carbon monoxide represents the lack of total conversion of glycerol during

the reforming process. Moreover, this is an indication of the meager activity of the water-gas shift reaction.

In this experiment (Figure 4.11), carbon monoxide selectivity had a maximum value of 59 % at a temperature of 275 ^{o}C and a minimum value of 37.8 % at 400 ^{o}C. These values are in good agreement with favorable kinetics for the WGS reaction at higher temperatures. Ironically, during aquouse phase reforming, applying a voltage reduced the CO selectivity suggesting that introduction of electrical charges makes system thermodynamics dominate even though kinetics are not that favorable for the WGS reaction at low temperatures. Again, the effect of electrical charges seemed to diminish during higher temperature gas-phase reforming.

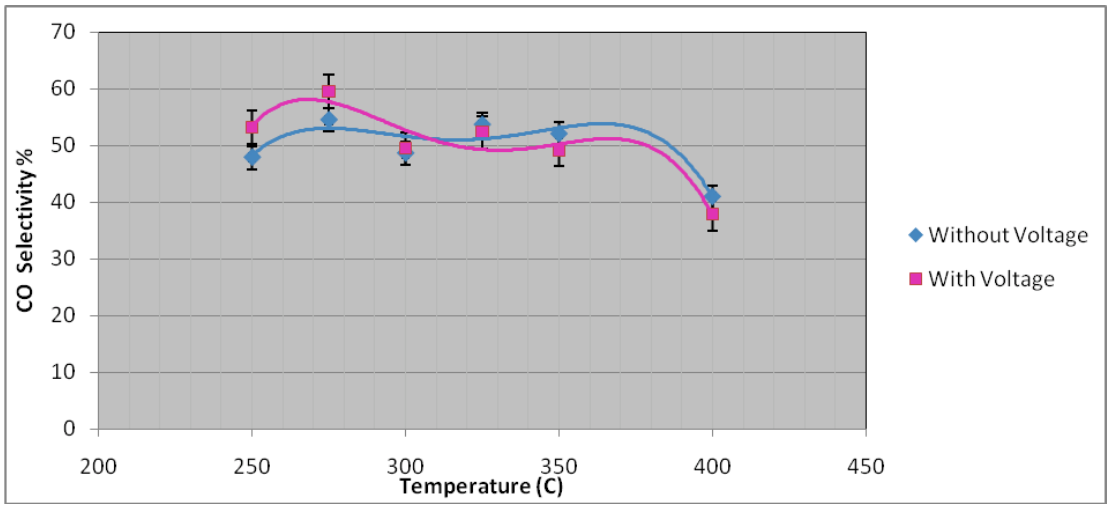

Figure 4.11 Effect of electrical charge and temperature on carbon monoxide selectivity

Results evince that carbon monoxide selectivity has been reduced by applied voltage at lower temperatures. This means that charged nanodroplets has enhanced the glycerol reforming process (this could be reinforced by cross referencing at hydrogen selectivities in figures 4.7, 4.9, and 4.10). The statistical analysis with split plot design suggests that CO selectivity is a quartic function of temperature for this experiment.

4.2.2.3 Effect of electrical charge and temperature on carbon dioxide selectivity

Carbon dioxide is the major co-product of glycerol reforming and gives valuable information on the quality of the reforming process as well as the substrate conversion effectiveness. During the first part of the experiment, it was evident that an applied voltage reduces the CO_2 selectivity at lower temperatures as compared to reforming non-charged substrate. At this point, it is difficult to pinpoint the exact reason behind this observation. However, the CO_2 selectivity was more or less identical for gas phase reforming regardless of whether the substrates were charged or not. One possible explanation is that charged glycerol increases methanation that in turn reduces CO_2 selectivity. Figure 4.12 depicts the quartic behavior of selectivity with respect to temperature.

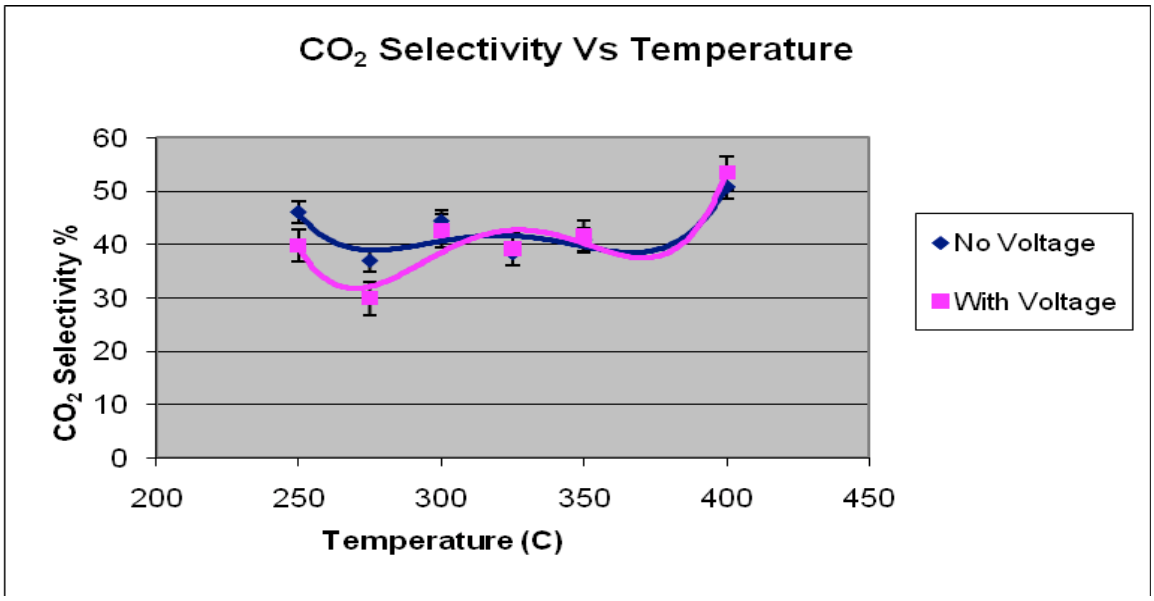

Figure 4.12 Effect of electrical charge and temperature on carbon dioxide selectivity

CO_2 selectivity reached a maximum at 400 ^oC which is 53 % while the minimum was 29 % at 275 ^oC, interestingly both these values were obtained when glycerol reforming was performed on charged nano droplets.

4.2.2.4 Effect of electrical charge and temperature on methane selectivity

Reduced carbon dioxide selectivity suggests that methane selectivity should increase as methantion occurs at lower temperatures. This is an undesired situation for charged nanodroplet reforming process. Figure 4.13 shows the methane selectivity variation with temperature. Methane selectivity has a maximum of 10 % at temperature 275 ^oC and a maximum increase in selectivity was found to be 30 % at 350 ^oC.

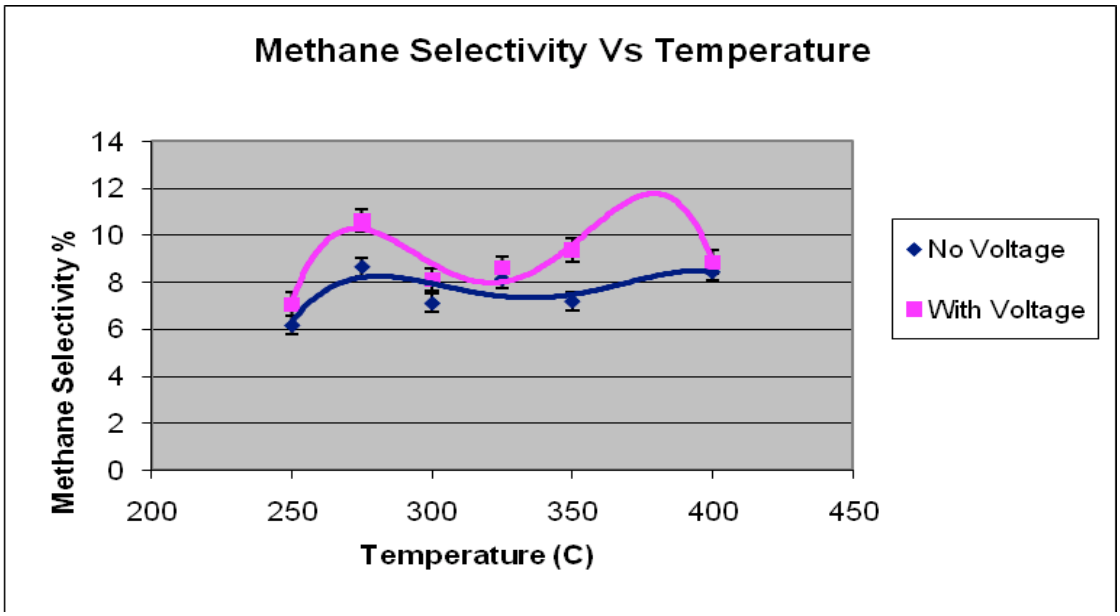

Figure 4.13 Effect of electrical charge and temperature on methane selectivity

The statistical analysis suggested a quartic behavior for selectivity with respect to temperature, for illustrative purposes the trend is depicted using a quadratic line. Figure 4.14 shows the quadratic behavior of methane selectivity with respect to temperature.

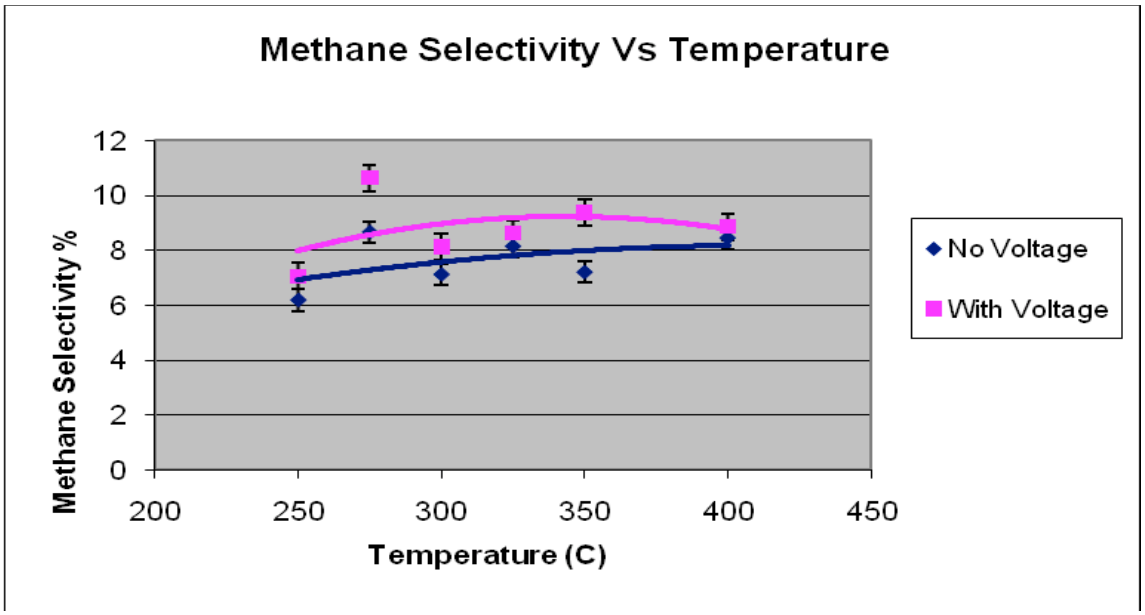

Figure 4.14 Effect of electrical charge and temperature on methane selectivity with quadratic trend line

Overall, an applied high voltage/charge had a definite impact on gas selectivities. Charged glycerol nanodroplets (despite being liquid/gas phase) had a positive effect on glycerol reforming than conventional reforming. Although the major goal of this experiment was to enhance the hydrogen selectivity of glycerol reforming process, it could be mentioned that when compared with all the other products, the overall performance of the process has been improved.

An overlay of increase of selectivity of four gases products from reforming charged and non-charged substrates is shown in Figure 4.15. Here, it is evident that the reforming process has been significantly enhanced when using charged substrates as opposed to non-charged substrates. The increase in gas selectivity as a percentage to the original value is shown in figure 4.16 for increased clarity.

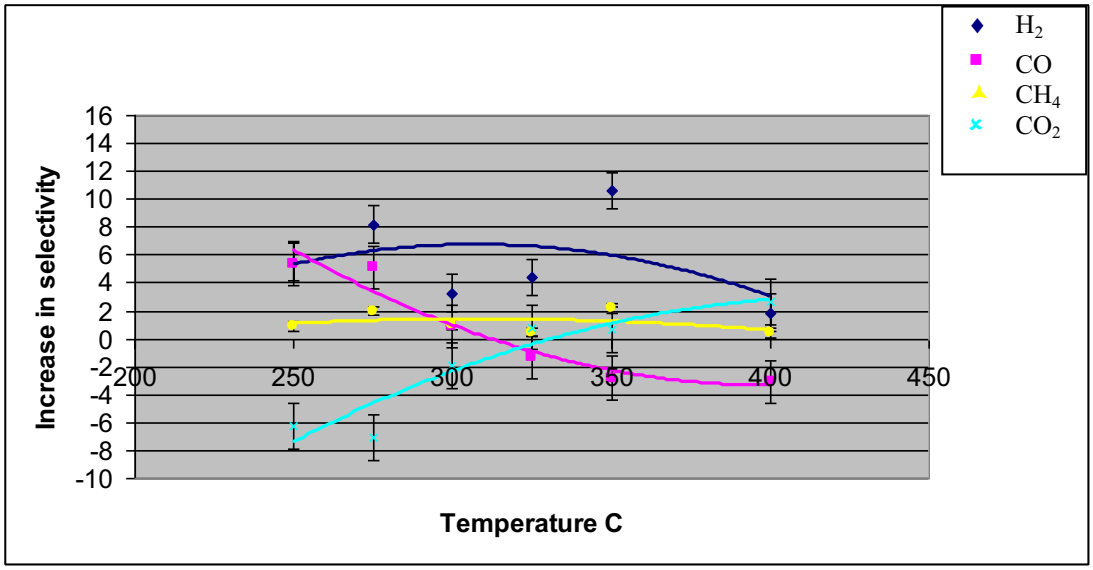

Figure 4.15 The net increase of gas selectivity between charged and non-charged substrate reforming

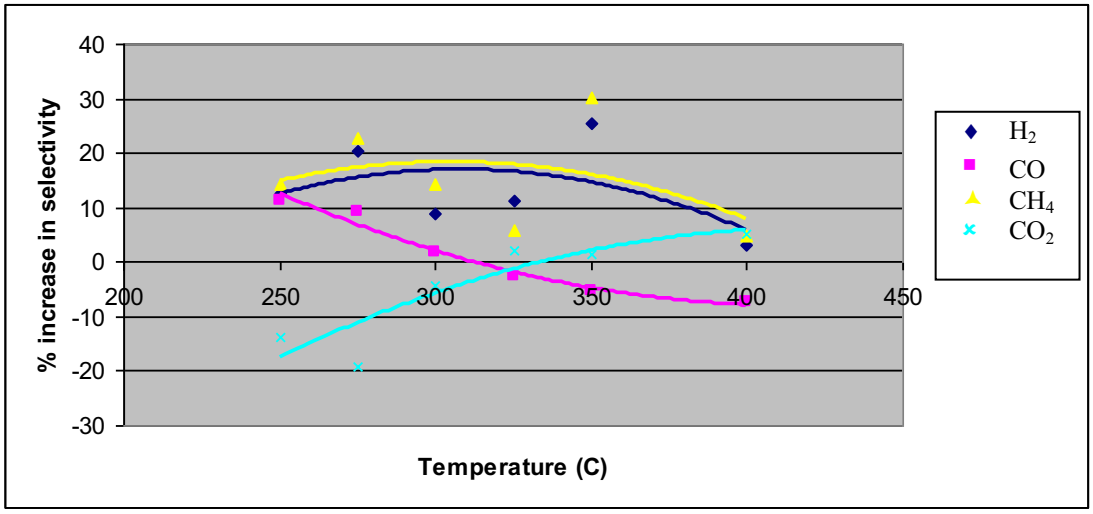

Figure 4.16 The increase in gas selectivity of charged substrate reformate as a percent of the non-charged value

4.2.3 Effect of electrical charge and temperature on glycerol conversion

It has been reported that steam reforming of glycerol has achieved more than 90 % conversion during certain experiments [46, 50] and with the aqueous phase reforming it has been reported to reach 99 % [24, 44, 66] under high pressure. This study was not geared towards maximizing glycerol conversion. In fact, in order to do objective comparisons, an operating range that fell far below maximum possible conversion has to be selected. In this exploratory study, a maximum conversion was achieved at 400 ^{o}C with 32.7 % in the presence of charged substrates. Overall glycerol conversion was around 15-20 % throughout the experiment. It was evident according to Figure 4.17 that the reforming charged substrates increased glycerol conversion across all temperatures.

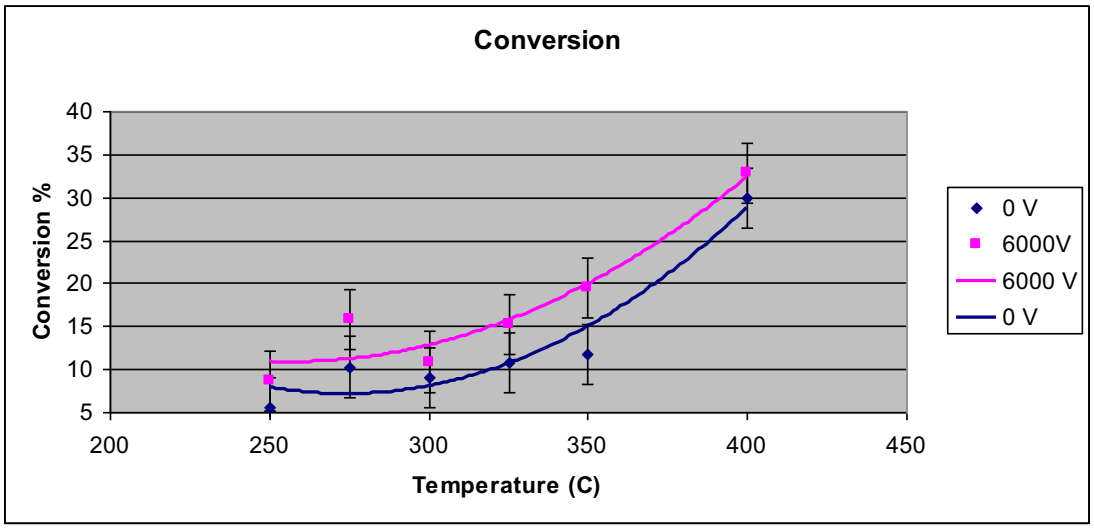

Figure 4.17 Effect of electrical charge and temperature on glycerol conversion

4.3 Voltage Dependency of Glycerol Reforming

Subsequent to the results obtained during the first phase, a second set of experiments were conducted to observe the effect of voltage (the amount of charge) on the effectiveness of liquid/gas phase reforming of glycerol. The chosen experimental temperature was 350 ^{o}C, and flow rate was kept constant at 0.004 ml/min. In this second phase, gas yields, selectivity and the conversion with respect to the voltage applied were analyzed.

4.3.1 Effect of voltage on gas yield

Figure 4.18 reports results of individual gas yields with varying voltages across the substrate steam and grounded conductive catalyst. It is clear that increasing voltage had a proportionately positive impact on hydrogen yield. The CO_2 yield remained relatively flat whereas the CO yield decreased with increasing voltage. CH_4 yield proportionately reduced with increasing voltage.

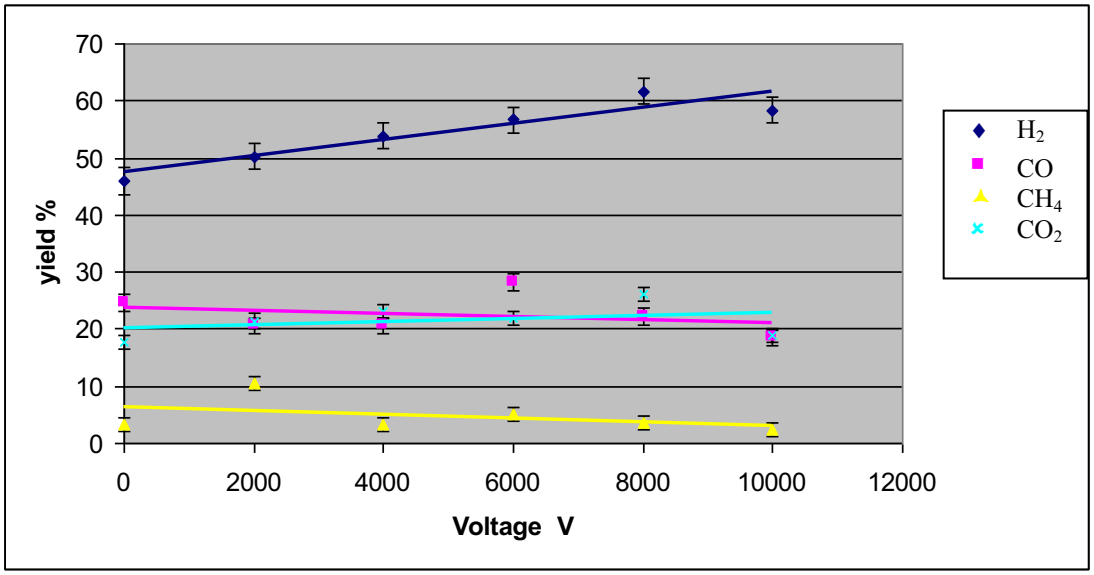

Figure 4.18 The effect of voltage on yields of various reformate gases

These results clearly indicate that reforming charged substrates enhances the effectiveness of the reforming reaction and increasing the amount of charges proportionately increase hydrogen yields. These observations make a convincing case that the hypothesis of charged particles enhancing mass transport at the catalyst surface is valid.

A maximum hydrogen yield of 62% was observed at 8000 V while a minimum of 46% was observed under neutral conditions (without any voltage applied). It should be noted that the experiment was limited to 10kV due to design limitations of the equipment.

4.3.2 Effect of voltage on reformate gas selectivity

Selectivity is a more accurate measure of the effectiveness of the reforming process. It is evident from Figure 4.19 that hydrogen selectivity has proportionately increased with increasing voltage. A maximum hydrogen selectivity of 53.7% was achieved at 8000 V. At 10,000 V hydrogen selectivity seemed to level off around 53%. Further studies should be carried out to affirm this observation. A minimum hydrogen selectivity of 38.5% was observed at neutral conditions.

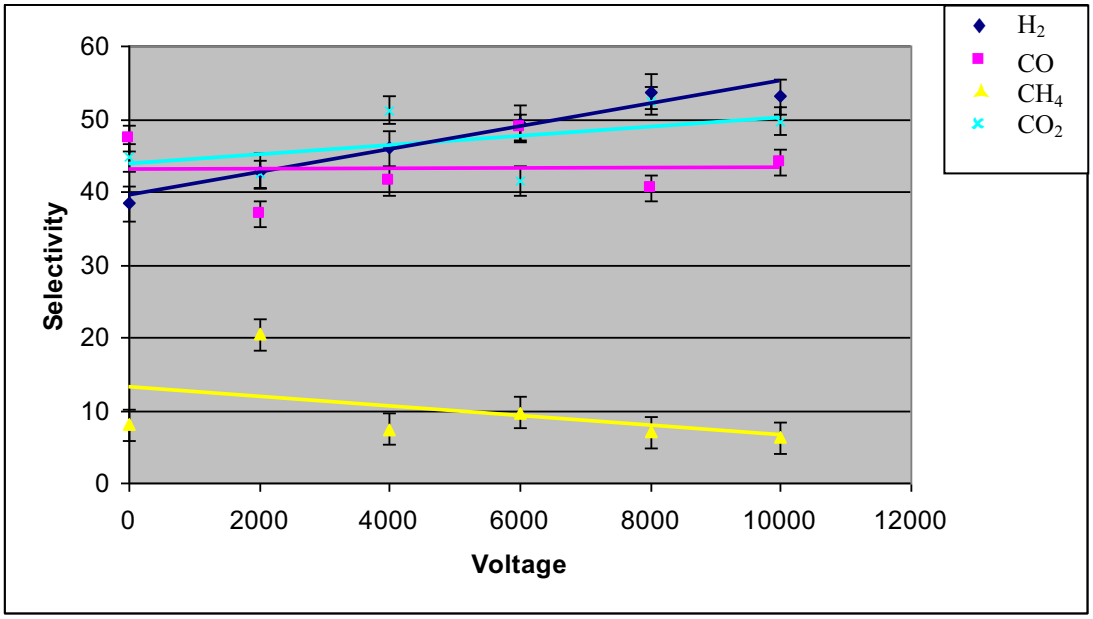

Figure 4.19 The effect of voltage on selectivity of various reformate gases

It is evident that according to figures 4.18 and figure 4.19 the trends of selectivity closely follow those of yields. The observations suggest that increasing

voltage favored reforming and water gas shift were as conditions disfavored methanation. Figure 4.20 depicts the percentage increase in hydrogen selectivity with respect to the increased voltage. It was evident that a 40 % increase in hydrogen selectivity was obtained when 8000 V was applied across the reaction bed as opposed to neutral conditions.

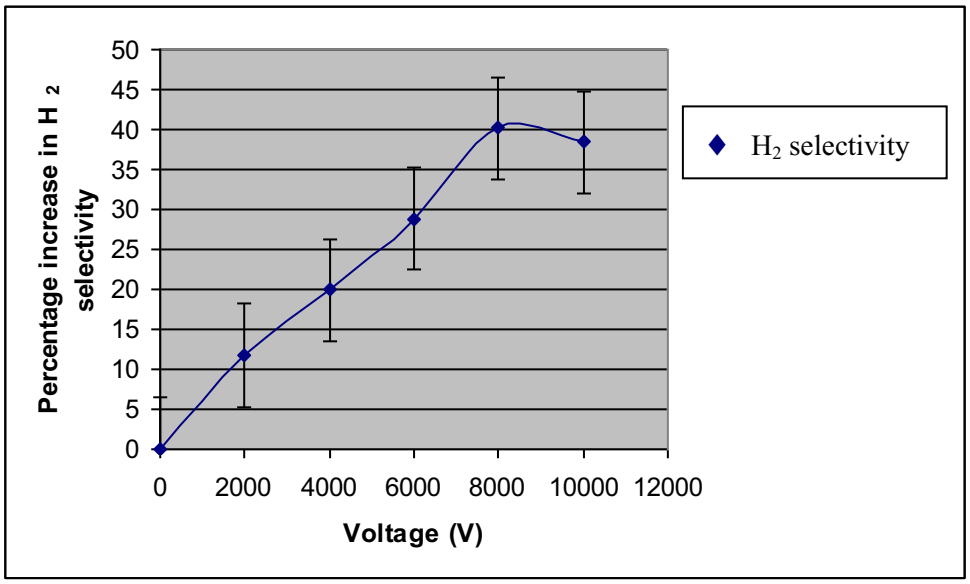

Figure 4.20 Percentage increase in hydrogen selectivity with respect to varying voltage across the substrate steam and conductive catalyst

Here is it increasingly evident that an increased voltage favored hydrogen selectivity. Again the advantages of charged substrate reforming seem to level off around 8kV potential difference.

4.4 Conclusions and Recommendations

From the first experiment we observed that enhanced gas yields were obtainable when electrosplit glycerol droplets were subjected to reforming. Hydrogen yield increase by 20 % at 350 ^{o}C when the substrate was electrospilt. However, the increase was negligible when the reforming temperature was increased to 400 ^{o}C. It was evident that throughout the whole temperature range tested, the H_2 yield increased when liquid feed was subjected to electro-spray (as opposed to gas phase reforming). Similarly, the CO_2 yield increased when the electrosplit substrate was reformed. A maximum of 18 % increase was observed at 350 ^{o}C and a miniscule 0.4 % increase was observed at 400 ^{o}C. Meanwhile, the CO and CH_4 yields also increased when electrosplit substrate was reformed. The glycerol conversion was also notably increased. Similarly hydrogen selectivity increased to a maximum of 25 % when electrosplit glycerol was reformed. The CO selectivity reduced when the substrate was electrosplit glycerol. It was noted that methanation has been increased possibly due to low pressure and temperature. It was observed that CO_2 and CH_4 selectivities improved due to electro-spray reforming. When considering all these observations, it is evident that reforming charged glycerol particles significantly enhances hydrogen yield and selectivity in aqueous phase and gas phase reforming. However, the positive effects of reformate charging diminished at high temperature gas phase reforming.

A significant drop in hydrogen yield and selectivity was observed around the boiling point of glycerol irrespective of reforming charged or neutral substrate.

Results from the second part of the experiment suggest that, when the magnitude of the applied voltage increases, the H_2 yield increased while CO and CO_2 had only a modest change. However methane selectivity was drastically reduced. Similarly, when the applied voltage was increased from 0 to 10,000 V, H_2 and CO_2 selectivities increased while CH_4 decreased drastically. Again CO yield didn't change due to an increase in the magnitude of the voltage. Possible reasons for the increase in H_2 selectivity may be higher voltage increasing the propensity to form a better electro-spray and/or enhanced transport phenomena due to charge attraction at the catalyst surface. More importantly the methane selectivity dropped with the increase of the applied voltage, which suggests that methanation reaction is hindered by an applied charge.

Finally, it is cautiously promising that feeding viscous substrate in the form of an electro-spray for an aqueous phase reforming enhances H_2 yield and selectivity. The results of this exploratory study favorably prove the hypothesis that reforming charged glycerol nanodroplets increase H_2 selectivity and glycerol conversion as opposed to reforming neutral substrate. Certainly further experimentation is needed to uncover the exact reasons behind these observations.

Moreover, elucidating the effect of pressure, correlation of the other experimental parameters such as temperature, voltage, feed flow rate and the type of catalyst on the efficacy of electro-spray reforming would be practically valuable future research directions to be explored.

REFERENCES

1. Abraham, S. (2002) *National Hydrogen Energy Road Map*. United State department of Energy.

2. Pagliaro, M. and M. Rossi, *The Future of Glycerol: New Uses of a Versatile Raw Material.* RSC Green Chemistry Book Series, 2008.

3. Dagle, R.A. and J.D. Holladay, *Methanol Steam Reforming for Hydrogen Production.* American Chemical Society, 2007. **107**(10): p. 3992-4022.

4. Haryanto, A., et al., *Current Status of Hydrogen Production Techniques by Steam Reforming of Ethanol: A Review.* Journal of Energy & Fuels, 2005. **19** p. 2098-2106.

5. Cortright, R.D., *Hydrogen Generation from Biomass-Derived Carbohydrates via the Aqueous-Phase Reforming (APR) Process*, in *Department of Energy Hydrogen Program*. 2005.

6. Cortright, R.D., *Hydrogen Generation from Biomass-Derived Carbohydrates via Aqueous-Phase Reforming Process.* Department of Energy Hydrogen Program, 2006.

7. Dunn, S., *Hydrogen futures: toward a sustainable energy system.* International Journal of Hydrogen Energy, 2002. **27**: p. 235–264.

8. Luo, N., et al., *Thermodynamic Study on Hydrogen Generation from Different Glycerol Reforming Processes.* Journal of Energy & Fuels, 2007. **21**: p. 3505–3512.

9. Adhikari, S. and S. Fernando, *Hydrogen Membrane Separation Techniques.* Industrial & Engineering Chemistry Research (This publication was among the most accessed articles published by American Chemical Society in 2006; number 1 most accessed journal article in Hydrogen Category in the 1st quarter of 2006 in the journal), 2006. **45**(3): p. 875-881.

10. NREL. 2006 [cited 2006; Available from: http://www.nrel.gov/.

11. Cortright, R.D., R.R. Davda, and J.A. Dumesic, *Hydrogen from Catalytic Reforming of Biomass-derived Hydrocarbons in Liquid Water.* Nature, 2002. **418**: p. 964-966.

12. Deluga, G.A., et al., *Renewable Hydrogen from Ethanol by Autothermal Reforming.* Science Asia, 2004. **303**(5660): p. 993-997.

13. Adhikari, S. and S. Fernando. *Glycerin Steam Reforming for Hydrogen Production*. in *Proceedings of the International Symposium on Hydrogen from Renewable Sources and Refinery Applications*. 2006. Atlanta, Georgia, USA Americal Chemical Society.

14. Czernik, S., et al., *Hydrogen by Catalytic Steam Reforming of Liquid Byproducts from Biomass Thermoconversion Process.* Industrial & Engineering Chemistry Research, 2002. **41**: p. 4209-4215.

15. Hirai, T., et al., *Production of Hydrogen by Steam Reforming of Glycerin on Ruthenium Catalyst.* Energy & Fuels, 2005. **19**: p. 1761-1762.

16. Davda, R.R., et al., J. A., Appl. Catal., 2002. **B 43**(13).

17. Davda, R.R., Dumesic, J. A., Ang. Chem. Int. Ed, 2003. **42**: p. 4068.

18. Shabaker, J.W., et al., J. Catal., 2003. **215**: p. 344.

19. Shabaker, J.W., et al., J.A. Catal. Lett, 2003. **88**(1).

20. King, D., et al. *Production of Hydrogen by Biomass Reforming*. 2005; Available from: www.hydrogen.energy.gov/pdfs/review05/pd6_king.pdf.

21. Yadav, G.D. and A.D. Murkute, *Kinetics of Synthesis of Perfumery Grade p-tert-Butylcyclohexyl Acetate Over Ion Exchange Resin Catalyst* International Journal of Chemical Reactor Engineering, 2003. **1**.

22. Boreskov, G.K., *Heterogeneous Catalysis*. Translation from Russian ed. K.I. Zamaraev and A.V. Khasin: Boreskov Institute of Catalysis, Russia.

23. J.W, S., et al., *Aqueous-phase reforming of methanol and ethylene glycol over alumina-supported platinum catalysts*, in *Journal of Catalysis*. 2003. p. 344–352.

24. Shabaker, J.W., G.W. Huber, and J.A. Dumesic, *Aqueous-phase reforming of oxygenated hydrocarbons over Sn-modified Ni catalysts.* Journal of Catalysis, 2004 **222**: p. 180–191.

25. Liao, C. *The Effect of passive Mixing in Steam-reformation*. 2006; Hydrogen Production & Utilization Laboratory, Mechanical & Aeronautical Engineering, Institute of Transportation Studies, University of California-Davis].

26. Vernon, D. *Heat Transfer Limitations in Hydrogen Production via Steam Reformation*. 2006; Hydrogen Production & Utilization Laboratory, Mechanical & Aeronautical Engineering, Institute of Transportation Studies, University of California-Davis].

27. Erickson, P.A., et al. *Space Velocity as an Insufficient Parameter in the Steam-Reforming Process*. in *From Proceeding (448) Power and Energy Systems* 2004.

28. Fitzgerald, S.P., et al. *A Compact Steam Reforming Reactor for Use in an Automotive Fuel Processor*. 2006 [cited 2006 09/08/2006].

29. Breithaupt, J., *New Understanding Physics for Advanced Level* 4th ed. 2000: Nelson Thornes.

30. NASA. [cited 2006 09/08/2006]; Available from: http://www.lerc.nasa.gov/WWW/K-12/airplane/state.html.

31. Duncan, T., *GCSE Physics*. 2000: Jim Murray Publisher.

32. Gaskell, S.J., *Electrospray : Principles and Practice.* JOURNAL OF MASS SPECTROMETRY, 1997. **32**: p. 677-688.

33. Orme, M., *Experiments on Droplet Collisions, Bounce, Coalescence and Disruption.* Progress in Energy and Combustion Science, 1997. **23**: p. 65-79.

34. Wilemski, G. and J.-S. Li. *Theoretical Studies of Nano Droplet Formation and Microstructure*. in *Proceedings of the Twentieth Symposium on Energy Engineering Sciences, Argonne IL, May 2002 (OSTI, CONF-2002)*. 2002.

35. Olumee, Z., J.H. Callahan, and A. Vertes, *Droplet Dynamic Changes in Electrostatic Sprays of Methanol-Water Mixtures.* J. Phys. Chem. A, 1998. **102** p. 9154-9160.

36. Zeleny, J., *Instability of electrified liquid surfaces.* Physical review, 1917. **10**: p. 1-6.

37. Gaskell, S.J., *Electrospray : Principles and Practice.* Journal of Mass Spectrometry, 1997. **32**: p. 677-688.

38. Tugnoli, A., G. Landucci, and V. Cozzani, *Sustainability assessment of hydrogen production by steam reforming.* International Journal of Hydrogen Energy, 2008. **33**: p. 4345-4357.

39. Chen, M., et al., *Long-term results of high-dose conformal radiotherapy for patients with medically inoperable T1-3N0 non-small-cell lung cancer: is low incidence of regional failure due to incidental nodal irradiation?* Int J Radiat Oncol Biol Phys, 2006. **64**(1): p. 120-6.

40. Dauenhauer, P.J., J.R. Salge, and L.D. Schmidt, *Renewable hydrogen by autothermal steam reforming of volatile carbohydrates.* Journal of Catalysis, 2006. **244**: p. 238–247.

41. Dumesic, J.A., et al., *Catalytic Production of Renewable Fuels by Aqueous-phase Reforming of Biomass-Derived Oxygenated Hydrocarbons.*

42. Liu, B., et al., *Hydrogen Generation from Glycerol via Aqueous Phase Reforming.* CFFS Annual Meeting, 2006.

43. Slinn, M., et al., *Steam reforming of biodiesel by-product to make renewable hydrogen.* Bioresource Technology, 2008. **99**: p. 5851–5858.

44. Luo, N., et al., *Thermodynamic analysis of aqueous-reforming of polylols for hydrogen generation.* Fuel, 2007. **86**: p. 1727–1736.

45. Hirai, T., et al., *Production of hydrogen by steam reforming of glycerin on Ruthenium catalyst.* Energy & Fuels, 2005. **19**: p. 1761-1762.

46. Adhikari, S., et al., *Conversion of Glycerol to Hydrogen via a Steam Reforming Process over Nickel Catalysts.* Energy & Fuels, 2008. **22** p. 1220–1226.

47. Adhikari, S., et al., *A thermodynamic analysis of hydrogen production by steam reforming of glycerol.* International Journal of Hydrogen Energy, 2007 **32**: p. 2875 – 2880.

48. Cortright, R.D., R.R. Davda, and J.A. Dumesic, *Hydrogen from catalytic reforming of biomass-derived hydrocarbons in liquid water.* Nature, 2002. **418**.

49. Murata, K., I. Takahara, and M. Inaba, *Propane formation by aqueous-phase reforming of glycerol over Pt/H-ZSM5 catalysts.* Journal of reaction kinetics 2008. **93**.

50. Luo, N., et al., *Glycerol aqueous phase reforming for hydrogen generation over Pt catalyst – Effect of catalyst composition and reaction conditions.* Fuel, 2008. **87**: p. 3483–3489.

51. Hayati, I., A.I. Bailey, and T.F. Tadros, *Effect of Electric Field and the Environment on Pendant Drops and Factors Affecting the Formation of Stable Jets and Atomization.* Journal of Colloid and Interface Science, 1987. **117**: p. 205-221.

52. Hayati, I., A. Bailey, and T.F. Tadros, *Mechanism of Stable Jet Formation and Electrical Forces Acting on a Liquid Gone.* Journal of Colloid and Interface Science, 1987. **117**: p. 222-230.

53. Jaworek, A., *Micro- and nanoparticle production by electrospraying.* Powder Technology, 2007. **176**: p. 18–35.

54. Krupa, A., et al., *Efficiency of particle charging by an alternating electric field charger.* Journal of Electrostatics, 2005 **63** p. 673–678.

55. Jaworek, A. and A.T. Sobczyk, *Electrospraying route to nanotechnology: An overview.* Journal of Electrostatics, 2007. **66**: p. 197-219.

56. Speranza, A., et al., *Electro-spraying of a highly conductive and viscous liquid.* Journal of Electrostatics, 2001. **51-52**: p. 494-501.

57. Ku, B.K. and S.S. Kim, *Electrospray characteristics of highly viscous liquids.* Journal of Aerosol Science, 2002. **33**: p. 1361–1378.

58. Marginean, I., et al., *Electrospray Characteristic Curves: In Pursuit of Improved Performance in the Nanoflow Regime.* American Chemical Society, 2007. **79**(21): p. 8030-8036.

59. Ku, B.K. and S.S. Kim, *Electrohydrodynamic spraying characteristics of glycerol solutions in vacuum.* Journal of Electrostatics, 2003. **57**: p. 109-128.

60. Marginean, I., P. Nemes, and A. Vertes, *A stable regime in electrosprays.* The American Physical Society, 2007. **76**.

61. Tsouris, C., et al., *Electrostatic Spraying of Nonconductive Fluids into Conductive Fluids.* AIChE Journal, 1994. **40**: p. 1920-1923.

62. Watanabea, H., T. Matsuyama, and H. Yamamoto, *Experimental study on electrostatic atomization of highly viscous liquids.* Journal of Electrostatics, 2003. **57**: p. 183-197.

63. Jaworek, A., et al., *Spectroscopic studies of electric discharges in electrospraying.* Journal of Electrostatics, 2005. **63**: p. 635–641.

64. Jaworek, A. and A. Krupa, *Studies of the corona discharge in ehd spraying.* Journal of Electrostatics, 1997. **40&41**: p. 173-178.

65. Adhikari, S., S. Fernando, and M. Novotny, *Nanoparticles production from glycerin via electrospray and size measurenment techniques*, in *American Society of Agricultural and Biological Engineers*. 2006. p. 1269-1272.

66. Boonyanuwat, A., A. Jentys, and J.A. Lercher, *Hydrogen production by aqueous-phase reforming of glycerin on noble supported catalysts*, in *DGMK/SCI-Conference*. 2006.

67. Davda, R.R., et al., *Aqueous-phase reforming of ethylene glycol on silica-supported metal catalysts.* Applied Catalysis B: Environmental, 2003. **43**: p. 13-26.

68. Adhikari, S., S.D. Fernando, and A. Haryanto, *Glycerin steam reforming for hydrogen production*, in *American Society of Agricultural and Biological Engineers*. 2006. p. 591−595.

APPENDIX

S.A.S OUTPUT FOR SPLIT PLOT EXPERIMENTAL DESIGN ON HYDROGEN, CARBON MONOXIDE, CARBON DIOXIDE, METHANE DATA

HYDROGEN DATA

The GLM Procedure

Class Level Information

Class	Levels	Values
cat_load	3	1 2 3
voltage	2	N Y
temperature	6	250 275 300 325 350 400

Number of Observations Read	36
Number of Observations Used	36

The GLM Procedure

Dependent Variable: selectivity

Source	DF	Sum of Squares	Mean Square	F Value	Pr > F
Model	15	2542.064607	169.470974	2.67	0.0208
Error	20	1267.764307	63.388215		
Corrected Total	35	3809.828914			

R-Square	Coeff Var	Root MSE	selectivity Mean
0.667239	16.97335	7.961672	46.90691

Source	DF	Type I SS	Mean Square	F Value	Pr > F
cat_load	2	79.073788	39.536894	0.62	0.5460
voltage	1	409.031008	409.031008	6.45	0.0195
cat_load*voltage	2	23.574817	11.787409	0.19	0.8317
temperature	5	1847.187478	369.437496	5.83	0.0018
voltage*temperature	5	183.197516	36.639503	0.58	0.7163

Source	DF	Type III SS	Mean Square	F Value	Pr > F
cat_load	2	79.073788	39.536894	0.62	0.5460
voltage	1	409.031008	409.031008	6.45	0.0195

cat_load*voltage	2	23.574817	11.787409	0.19	0.8317
temperature	5	1847.187478	369.437496	5.83	0.0018
voltage*temperature	5	183.197516	36.639503	0.58	0.7163

Contrast	DF	Contrast SS	Mean Square	F Value	Pr > F
linear	1	503.720237	503.720237	7.95	0.0106
Quad	1	1059.797183	1059.797183	16.72	0.0006
CUBIC	1	168.513923	168.513923	2.66	0.1186
quartic	1	72.717695	72.717695	1.15	0.2969
quintic	1	42.438440	42.438440	0.67	0.4229

Tests of Hypotheses Using the Type III MS for cat_load*voltage as an Error Term

Source	DF	Type III SS	Mean Square	F Value	Pr > F
cat_load	2	79.0737876	39.5368938	3.35	0.2297
voltage	1	409.0310079	409.0310079	34.70	0.0276

The GLM Procedure

t Tests (LSD) for selectivity

NOTE: This test controls the Type I comparisonwise error rate, not the experimentwise error rate.

Alpha	0.05
Error Degrees of Freedom	20
Error Mean Square	63.38822
Critical Value of t	2.08596
Least Significant Difference	9.5885

Means with the same letter are not significantly different.

t Grouping	Mean	N	temperature
A	61.118	6	400
B	47.748	6	275
B			
B	47.113	6	350
B			
B	45.881	6	250
B			
B	40.981	6	325
B			
B	38.600	6	300

The GLM Procedure

t Tests (LSD) for selectivity

NOTE: This test controls the Type I comparisonwise error rate, not the experimentwise error rate.

Alpha	0.05
Error Degrees of Freedom	2
Error Mean Square	11.78741
Critical Value of t	4.30265
Least Significant Difference	4.9241

Means with the same letter are not significantly different.

t Grouping	Mean	N	voltage
A	50.278	18	Y
B	43.536	18	N

CARBON MONOXIDE DATA

The GLM Procedure

Class Level Information

Class	Levels	Values
cat_load	3	1 2 3
voltage	2	N Y
temperature	6	250 275 300 325 350 400

Number of Observations Read	36
Number of Observations Used	36

The GLM Procedure

Dependent Variable: selectivity

Source	DF	Sum of Squares	Mean Square	F Value	Pr > F
Model	15	2275.572697	151.704846	4.50	0.0011
Error	20	673.824385	33.691219		

Corrected Total	35	2949.397082	

R-Square	Coeff Var	Root MSE	selectivity Mean
0.771538	11.62951	5.804414	49.91107

Source	DF	Type I SS	Mean Square	F Value	Pr > F
cat_load	2	1089.951418	544.975709	16.18	<.0001
voltage	1	4.304706	4.304706	0.13	0.7245
cat_load*voltage	2	40.600876	20.300438	0.60	0.5571
temperature	5	1033.162433	206.632487	6.13	0.0013
voltage*temperature	5	107.553265	21.510653	0.64	0.6730

Source	DF	Type III SS	Mean Square	F Value	Pr > F
cat_load	2	1089.951418	544.975709	16.18	<.0001
voltage	1	4.304706	4.304706	0.13	0.7245
cat_load*voltage	2	40.600876	20.300438	0.60	0.5571
temperature	5	1033.162433	206.632487	6.13	0.0013
voltage*temperature	5	107.553265	21.510653	0.64	0.6730

Contrast	DF	Contrast SS	Mean Square	F Value	Pr > F
LINEAR	1	433.5399306	433.5399306	12.87	0.0018
QUARD	1	310.0101854	310.0101854	9.20	0.0066
CUBIC	1	23.9571248	23.9571248	0.71	0.4091
quartic	1	178.9761072	178.9761072	5.31	0.0320
quintic	1	86.6790847	86.6790847	2.57	0.1244

Tests of Hypotheses Using the Type III MS for cat_load*voltage as an Error Term

Source	DF	Type III SS	Mean Square	F Value	Pr > F
cat_load	2	1089.951418	544.975709	26.85	0.0359
voltage	1	4.304706	4.304706	0.21	0.6904

The GLM Procedure

t Tests (LSD) for selectivity

NOTE: This test controls the Type I comparisonwise error rate, not the experimentwise error rate.

Alpha	0.05
Error Degrees of Freedom	20
Error Mean Square	33.69122

Critical Value of t	2.08596
Least Significant Difference	6.9904

Means with the same letter are not significantly different.

t Grouping		Mean	N	temperature
	A	56.994	6	275
	A			
B	A	52.958	6	325
B	A			
B	A	50.589	6	350
B	A			
B	A	50.543	6	250
B				
B		49.010	6	300
	C	39.372	6	400

The GLM Procedure

t Tests (LSD) for selectivity

NOTE: This test controls the Type I comparisonwise error rate, not the experimentwise error rate.

Alpha	0.05
Error Degrees of Freedom	2
Error Mean Square	20.30044
Critical Value of t	4.30265
Least Significant Difference	6.462

Means with the same letter are not significantly different.

t Grouping	Mean	N	voltage
A	50.257	18	Y
A			
A	49.565	18	N

CARBON DIOXIDE DATA

The GLM Procedure

Class Level Information

Class	Levels	Values
cat_load	3	1 2 3
voltage	2	N Y
temperature	6	250 275 300 325 350 400

Number of Observations Read	36
Number of Observations Used	36

The GLM Procedure

Dependent Variable: selectivity

Source	DF	Sum of Squares	Mean Square	F Value	Pr > F
Model	15	2192.666990	146.177799	3.12	0.0095
Error	20	938.275394	46.913770		
Corrected Total	35	3130.942384			

R-Square	Coeff Var	Root MSE	selectivity Mean
0.700322	16.34710	6.849363	41.89957

Source	DF	Type I SS	Mean Square	F Value	Pr > F
cat_load	2	862.967164	431.483582	9.20	0.0015
voltage	1	30.652989	30.652989	0.65	0.4284
cat_load*voltage	2	47.772037	23.886019	0.51	0.6086
temperature	5	1131.049680	226.209936	4.82	0.0047
voltage*temperature	5	120.225119	24.045024	0.51	0.7636

Source	DF	Type III SS	Mean Square	F Value	Pr > F
cat_load	2	862.967164	431.483582	9.20	0.0015
voltage	1	30.652989	30.652989	0.65	0.4284

cat_load*voltage	2	47.772037	23.886019	0.51	0.6086
temperature	5	1131.049680	226.209936	4.82	0.0047
voltage*temperature	5	120.225119	24.045024	0.51	0.7636

Contrast	DF	Contrast SS	Mean Square	F Value	Pr > F
linear	1	354.2738716	354.2738716	7.55	0.0124
Quad	1	364.3909908	364.3909908	7.77	0.0114
CUBIC	1	3.5131652	3.5131652	0.07	0.7872
quartic	1	268.6388336	268.6388336	5.73	0.0266
quintic	1	140.2328188	140.2328188	2.99	0.0992

Tests of Hypotheses Using the Type III MS for cat_load*voltage as an Error Term

Source	DF	Type III SS	Mean Square	F Value	Pr > F
cat_load	2	862.9671644	431.4835822	18.06	0.0525
voltage	1	30.6529890	30.6529890	1.28	0.3748

The GLM Procedure

t Tests (LSD) for selectivity

NOTE: This test controls the Type I comparisonwise error rate, not the experimentwise error rate.

Alpha	0.05
Error Degrees of Freedom	20
Error Mean Square	46.91377
Critical Value of t	2.08596
Least Significant Difference	8.2489

Means with the same letter are not significantly different.

t Grouping		Mean	N	temperature
	A	51.988	6	400
	B	43.383	6	300
	B			
	B	42.843	6	250
	B			
C	B	41.134	6	350
C	B			
C	B	38.672	6	325
C				
C		33.377	6	275

The GLM Procedure

t Tests (LSD) for selectivity

NOTE: This test controls the Type I comparisonwise error rate, not the experimentwise error rate.

Alpha	0.05
Error Degrees of Freedom	2
Error Mean Square	23.88602
Critical Value of t	4.30265
Least Significant Difference	7.0095

Means with the same letter are not significantly different.

t Grouping	Mean	N	voltage
A	42.822	18	N
A			
A	40.977	18	Y

METHANE DATA

The GLM Procedure

Class Level Information

Class	Levels	Values
cat_load	3	1 2 3
voltage	2	N Y
temperature	6	250 275 300 325 350 400

Number of Observations Read	36
Number of Observations Used	36

The GLM Procedure

Dependent Variable: selectivity

Source	DF	Sum of Squares	Mean Square	F Value	Pr > F
Model	15	67.0211276	4.4680752	0.98	0.5097

Error	20	91.4640517	4.5732026
Corrected Total	35	158.4851793	

R-Square	Coeff Var	Root MSE	selectivity Mean
0.422886	26.11319	2.138505	8.189365

Source	DF	Type I SS	Mean Square	F Value	Pr > F
cat_load	2	19.75369940	9.87684970	2.16	0.1415
voltage	1	11.98361408	11.98361408	2.62	0.1212
cat_load*voltage	2	0.29187559	0.14593780	0.03	0.9686
temperature	5	30.79826512	6.15965302	1.35	0.2856
voltage*temperature	5	4.19367345	0.83873469	0.18	0.9656

Source	DF	Type III SS	Mean Square	F Value	Pr > F
cat_load	2	19.75369940	9.87684970	2.16	0.1415
voltage	1	11.98361408	11.98361408	2.62	0.1212
cat_load*voltage	2	0.29187559	0.14593780	0.03	0.9686
temperature	5	30.79826512	6.15965302	1.35	0.2856
voltage*temperature	5	4.19367345	0.83873469	0.18	0.9656

Contrast	DF	Contrast SS	Mean Square	F Value	Pr > F
linear	1	3.99782962	3.99782962	0.87	0.3610
Quad	1	2.19609256	2.19609256	0.48	0.4963
CUBIC	1	9.12195628	9.12195628	1.99	0.1732
quartic	1	9.07220545	9.07220545	1.98	0.1743
quintic	1	6.41018121	6.41018121	1.40	0.2503

Tests of Hypotheses Using the Type III MS for cat_load*voltage as an Error Term

Source	DF	Type III SS	Mean Square	F Value	Pr > F
cat_load	2	19.75369940	9.87684970	67.68	0.0146
voltage	1	11.98361408	11.98361408	82.11	0.0120

The GLM Procedure

t Tests (LSD) for selectivity

NOTE: This test controls the Type I comparisonwise error rate, not the experimentwise error rate.

Alpha	0.05
Error Degrees of Freedom	20
Error Mean Square	4.573203
Critical Value of t	2.08596
Least Significant Difference	2.5755

Means with the same letter are not significantly different.

t Grouping		Mean	N	temperature
	A	9.629	6	275
	A			
B	A	8.639	6	400
B	A			
B	A	8.370	6	325
B	A			
B	A	8.276	6	350
B	A			
B	A	7.608	6	300
B				
B		6.614	6	250

The GLM Procedure

t Tests (LSD) for selectivity

NOTE: This test controls the Type I comparisonwise error rate, not the experimentwise error rate.

Alpha	0.05
Error Degrees of Freedom	2
Error Mean Square	0.145938
Critical Value of t	4.30265
Least Significant Difference	0.5479

Means with the same letter are not significantly different.

t Grouping	Mean	N	voltage
A	8.7663	18	Y
B	7.6124	18	N